Comparative analysis of Unmix/PMF modeling for $PM_{2.5}$ source apportionment in rural and urban Kansas and a review of life cycle assessment on carbon footprint of beef production

by

Yang Liu

B.S., Inner Mongolia Medical University, 2011
M.S., Kansas State University, 2013

AN ABSTRACT OF A DISSERTATION

submitted in partial fulfillment of the requirements for the degree

DOCTOR OF PHILOSOPHY

Department of Biological and Agricultural Engineering
College of Engineering

KANSAS STATE UNIVERSITY
Manhattan, Kansas

2018

Abstract

The Unmix and Positive Matrix Factorization (PMF) models for source apportionment were applied to evaluate prescribed burning impacts on air quality, identify model advantages, and establish a relationship between visibility and $PM_{2.5}$ sources. Speciated $PM_{2.5}$ data were from the Flint Hills (FH) rural and the Kansas City (KC) urban sites. At the FH site, the Unmix model identified five sources: nitrate/agricultural, sulfate/industrial, crustal/soil, smoke, and secondary organic aerosol (SOA); while the PMF model identified the copper source in addition. The smoke source from PMF result includes both primary and secondary aerosols from prescribed burning when the smoke source in Unmix result only includes primary burning aerosols. The secondary smoke aerosols at the FH site were combined with secondary aerosols from other origins and formed the SOA source in Unmix result. Comparative analysis of the modeling results estimated the SOA to be 2.3 to 2.7 times of the primary aerosols in burning season. At the KC site, both receptor models derived seven-source solutions: nitrate/agricultural, sulfate/industrial, crustal/soil, smoke, traffic/SOA, heavy-duty diesel vehicle (HDDV), and calcium. The smoke source at the KC site carries an exceedingly organic carbon to elemental carbon (OC/EC) ratio, which is more than five times higher than in FH smoke source. The PMF results at KC site tend to classify more SOA from nitrate/agricultural and sulfate/industrial sources into traffic/SOA source. In the burning season, the smoke source from both sites showed a relatively high correlation when KC is under west and southwest wind, suggesting that part of the smoke originated $PM_{2.5}$ at the urban site could be from the upwind burning activities. The Tobit modeling recognized the nitrate/agricultural as the leading visibility degradation impact factor at both sites.

The latter chapter conducted a review of life cycle assessment (LCA) on carbon footprint (CF) of beef production. The objectives were to evaluate CF range in raising systems from different

countries, identify the leading CF contributor and dominant source of uncertainty, and summarize LCA inventory defined in cattle production systems. Most existing beef LCA studies followed a "cradle to farm gate" approach. The CF in 3-phase systems ranged from 16 to 29.5 kg CO_2e kg^{-1} carcass weight. The 2-phase raising system reported a slightly lower CF than the 3-phase system (18.9 to 26.9 kg CO_2e kg^{-1} carcass weight), but no significant differences were observed. The grass-fed system in the US has the highest CF, but the CF of grass-fed systems in the European Union (EU) is 40% less than them in the US. This is because more than half of cattle farms in EU produce both beef and milk, and the CF burden was partaken by the dairy production. Cow-calf phase contributed the most CF in 3-phase raising system, while enteric fermentation was the major contributor. Feed production contributed the most in the feedlot phase if forages were applied rather than concentrates. The leading uncertainty sources reported was land use change and disparate dressing percentage. To improve the LCA accuracy, more research is needed in collecting reliable LCA inventory data such as raising period and feed intake efficiency.

Comparative analysis of Unmix/PMF modeling for $PM_{2.5}$ source apportionment in rural and urban Kansas and a review of life cycle assessment on carbon footprint of beef production

by

Yang Liu

B.S., Inner Mongolia Medical University, 2011
M.S., Kansas State University, 2013

A DISSERTATION

submitted in partial fulfillment of the requirements for the degree

DOCTOR OF PHILOSOPHY

Department of Biological and Agricultural Engineering
College of Engineering

KANSAS STATE UNIVERSITY
Manhattan, Kansas

2018

Approved by:

Major Professor
Zifei Liu

Copyright

Abstract

The Unmix and PMF models were applied for source apportionment to evaluate prescribed burning impacts, identify model advantages, and establish a relationship between visibility and $PM_{2.5}$ sources. Speciated $PM_{2.5}$ data were from the Flint Hills (FH) rural site and the Kansas City (KC) urban site. At the FH site, Unmix identified five sources: nitrate/agricultural, sulfate/industrial, crustal/soil, smoke, and secondary organic aerosol (SOA); while the PMF result identified the copper source in addition. The smoke source from PMF result includes both primary and secondary aerosols from prescribed burning when the smoke source in Unmix result only includes primary burning aerosols. The secondary smoke aerosols at the FH site were combined with secondary aerosols from other origins and formed the SOA source in Unmix result. Comparative analysis of the modeling results estimated the SOA in burning season, which is about 1.6 times higher than the primary aerosols. At the KC site, both receptor models derived seven-source solutions: nitrate/agricultural, sulfate/industrial, crustal/soil, smoke, traffic/SOA, heavy-duty diesel vehicle (HDDV), and calcium source. The smoke source at the KC site carries an exceedingly high OC/EC ratio, which is more than five times higher than in FH smoke source. The PMF results at KC site tend to classify more SOA from nitrate/agricultural and sulfate/industrial sources into traffic/SOA source. In burning season, the smoke source from both sites carried a relatively high correlation when KC is under west and southwest wind, suggesting that part of the smoke originated $PM_{2.5}$ at the urban site could be from the upwind burning activities. The Tobit modeling recognized the nitrate/agricultural as the leading visibility degradation impact factor at both sites.

The latter chapter conducted a review of life cycle assessment (LCA) on carbon footprint (CF) of beef production. The objectives were to evaluate CF range in raising systems from different

countries, identify the leading CF contributor and dominant source of uncertainty, and summarize LCA inventory defined in cattle production systems. Most existing beef LCA studies followed a "cradle to farm gate" approach. The CF in 3-phase systems ranged from 16 to 29.5 kg CO_2e kg^{-1} carcass weight. The 2-phase raising system reported a slightly lower CF than the 3-phase system (18.9 to 26.9 kg CO_2e kg^{-1} carcass weight), but no significant differences were observed. The grass-fed system in the US has the highest CF, but the CF of grass-fed systems in the European Union (EU) is 40% less than them in the US. This is because more than half of cattle farms in EU produce both beef and milk, and the CF burden was partaken by the dairy production. Cow-calf phase contributed the most CF in 3-phase raising system, while enteric fermentation was the major contributor. Feed production contributed the most in the feedlot phase if forages were applied rather than concentrates. The leading uncertainty sources reported was land use change and disparate dressing percentage. To improve the LCA accuracy, more research is needed in collection reliable LCA inventory data such as raising period and feed intake efficiency.

Table of Contents

List of Figures xi

List of Tables xiii

Acknowledgments xiv

Chapter 1 - Comparative analysis of Unmix/ PMF modeling for $PM_{2.5}$ source apportionment in rural and urban Kansas 1

1.1 Introduction 1

Objectives 3

1.2 Literature review 3

1.2.1 Unmix model applications 3

1.2.2 PMF model applications 5

1.2.3 Studies focused on the comparison of receptor model results 6

1.2.4 Existing visibility impairment studies 7

1.3 Methods 7

1.3.1 Sampling locations and data sources 7

1.3.2 Speciated $PM_{2.5}$ data sorting 9

1.3.3 Receptor model implementation 10

1.3.4 Visibility measurement and processing method 11

1.3.5 Temporal visibility variation analysis method 12

1.4 Results and discussion 12

1.4.1 The Flint Hills rural site 12

The Unmix model result 12

The PMF model result 19

Comparison of the Unmix and PMF modeling results at the Flint Hills site........ 26

1.4.2 The Kansas City urban site 28

The Unmix model result 28

The PMF model result 34

Comparison of Unmix and PMF modeling results at the Kansas City site 39

1.4.3 Site comparison.. 40

1.4.4 $PM_{2.5}$ source impacts on visibility degradation in rural and urban Kansas 43

Temporal variation of visibility 43

Effects of meteorological parameters on visibility 45

Tobit model and effects of $PM_{2.5}$ sources 46

1.5 Conclusions, limitation, and future work... 48

Chapter 2 - A review of life cycle assessment on the carbon footprint of beef production in the U.S. 51

2.1 Introduction... 51

Objectives 52

2.2 Database selection and literature search 52

2.3 Review of LCA inventory.. 54

2.3.1 LCA goal and scope 54

2.3.2 System boundaries and beef raising system.. 55

2.3.3 Method of allocation 57

2.3.4 Greenhouse gas emission assessment in LCA studies 58

2.4 Review and analysis of the Carbon footprint... 60

2.4.1 Function unit and dressing percentage.. 60

2.4.3 Carbon Footprint range and breakdowns 62

2.4.4 Sensitivity analysis and uncertainty analysis 69

2.5 Conclusions, limitation, and future work.. 70

References.. 72

List of Figures

Figure 1 NASA satellite image of burning activities in 2014 and locations of the speciated $PM_{2.5}$ sampling sites 8

Figure 2 Monthly source contribution from Unmix model result at the Flint Hills site 15

Figure 3 Time series of Flint Hills Unmix source contributions on $PM_{2.5}$ (dates are in m/d/y) ... 16

Figure 4 Monthly average source contribution from the PMF model result at the Flint Hills site 19

Figure 5 Time series of the Flint Hills PMF source contributions on $PM_{2.5}$ (dates are in m/d/y) 21

Figure 6 Monthly-averaged contributions of smoke-related sources from both models at the Flint Hills site 24

Figure 7 Monthly P4/U4 ratio at the Flint Hills site 25

Figure 8 Comparison of the Unmix and PMF results at the Flint Hills site 27

Figure 9 Monthly source contribution from the Unmix model result at the Kansas City site 30

Figure 10 Time series plots of selected Kansas City Unmix source contributions on $PM_{2.5}$ (dates are in m/d/y) 31

Figure 11 Monthly source contribution from the PMF model result at the Kansas City site 35

Figure 12 Monthly nitrate/agricultural $PM_{2.5}$ (in µg/m^3) comparison at the Kansas City site. 36

Figure 13 Monthly sulfate/industrial $PM_{2.5}$ (in µg/m^3) comparison at the Kansas City site 37

Figure 14 Comparison between Unmix and PMF results at the Kansas City site 40

Figure 15 Average contributions of selected categories (in µg/m^3) by wind directions........ 42

Figure 16 Smoke originated $PM_{2.5}$ (in µg/m^3) distributed by wind direction during the burning seasons. 42

Figure 17 Annual and diurnal visibility variation in Flint Hills and Kansas City 43

Figure 18 Scatter plots between ambient $PM_{2.5}$ and visibility from Flint Hills rural and Kansas City urban sites. 47

Figure 19 Geographic locations of LCA studies in the U.S. 54

Figure 20 Beef raising system and system boundaries from inclusive LCA studies.................... 56

Figure 21 Beef production carbon footprint under different raising systems in EU and US........ 66

List of Tables

Table 1 Flint Hills (FH) site Unmix model results-Source contribution and composition (µg/m^3) 13

Table 2 Pearson correlation coefficient of the Flint Hills Unmix sources and some species. 15

Table 3 Example of early July smoke source contributions to ambient $PM_{2.5}$ (µg/m^3) 18

Table 4 The FlintHills site PMF model results- Source contribution and composition (µg/m^3).. 20

Table 5 Pearson correlation coefficient matrix of the Flint Hills PMF sources and some species. 20

Table 6 The Kansas City site Unmix model results-Source contribution and composition (µg/m^3) 29

Table 7 Pearson correlation coefficient matrix of the Kansas City Unmix sources and some species. 30

Table 8 The Kansas City PMF results - Source contribution and composition (µg/m^3)) 34

Table 9 Visibility impact factor and parameter estimations in the Tobit model. 48

Table 10 Number of articles published each year in the databases, citing "Life Cycle Assessment", "carbon footprint", and "beef" in title, keywords or abstract. 53

Table 11 IPCC editions of greenhouse gases conversion to CO_2 equivalent 59

Table 12 Beef dressing percentage used in published carbon footprint studies 61

Table 13 Overview of carbon footprint range in published beef LCA studies outside U.S. 62

Table 14 Overview of carbon footprint range in published beef LCA studies in the U.S. 63

Table 15 CF breakdown from the literature based on beef production system 67

Acknowledgments

I would first express the deepest appreciation to my advisor Dr. Zifei Liu. Thank you for your continual encouragement on my research and being greatly supportive when I am working on the dissertation in a distance. Without your guidance and persistent help, this dissertation would not have been possible. I would like to thank Dr. Ronaldo Maghirang, Dr. Eduardo Santos, Dr. Weixing Song, and Dr. Doina Caragea for serving as my committee members, for the great support and invaluable advice.

Thanks to my mentors and colleagues at the K-State community: Dr. Chengappa, Dr. Rowland's lab, Dr. Nutsch, Dr. Harner, a special thanks goes to Barbara Moore from the BAE family. I want to thank you for all the opportunities I was given to conduct my research. Sincerely thanks to my friends at Manhattan, thank you for the continued patience and endless support. Nobody has been more important to me in pursuing this graduate program than the member of my family. I would like to thank my parents, whose love and guidance are with me in whatever I do. Most importantly, I would express appreciation to my loving husband Dr. Xi Chen, and son David Chen, who provide unending inspiration.

Chapter 1 - Comparative analysis of Unmix/ PMF modeling for $PM_{2.5}$ source apportionment in rural and urban Kansas

1.1 Introduction

Particulate pollution or $PM_{2.5}$ is a term for particles with an equivalent aerodynamic diameter equal or less than 2.5 micrometers. The rapid increasing ambient $PM_{2.5}$ in recent decades has become a major public health concern. High concentration of $PM_{2.5}$ has been associated with atmospheric environmental influence and serious adverse health effects (National Research Council, 1999).

The sources of ambient $PM_{2.5}$ were considered from a regional scale due to its tendency for long-range transport. In Kansas, the prescribed pasture burning is considered a major source of $PM_{2.5}$ in the region. The tallgrass prairie region covers 18 Kansas counties and roughly 7 million acres of rangeland, of which about 2 million acres are burned each year. There are many benefits of prescribed burning, such as controlling the growth of trees and weeds, releasing soil nutrients and helping revitalize the soil, eliminating pathogens that cause plant diseases, and preserving the high-quality grazing area for cattle. However, potential health hazards and environmental concerns are raised for both local and downwind regions.

The small particulates are able to remain airborne for weeks and can be transported over long distances (Kansas Department of Health and Environment, 2010). $PM_{2.5}$ that attach or absorb chemicals and toxins can penetrate the human respiratory system, and cause respiratory diseases or even fatal consequences. $PM_{2.5}$ is the main cause of visibility degradation, which affects the safety of all forms of traffic. The environmental effects of $PM_{2.5}$ are also related to soil acidification, eutrophication, etc. (Kansas Department of Health and Environment, 2010)

Prescribed burning in the Flint Hills region has been practiced for maintaining tallgrass prairie ecosystem for decades, it is usually conducted during a narrow window in late spring (Towne and Craine, 2014). In 2010, the Kansas Department of Health and Environment (KDHE) developed the Flint Hills Smoke Management Plan, which is the first step towards reducing the impacts of Flint Hills burning on air quality. Generally, the emissions and meteorological inputs were employed in the dispersion models to predict concentrations at selected downwind locations. Studies have attempted to quantifying the contributions of prescribed burning, however, the inadequacy of detailed local source profiles of burning has been a limitation for using dispersion modeling. Receptor models were recommended by the US EPA for identifying and quantifying the sources of air pollutants at a receptor location, without the use of meteorological data and chemical transformation mechanisms to estimate the contribution of sources to receptor concentrations (EPA, 2016). There are three commonly used receptor models: Chemical Mass Balance (CMB), Unmix, and Positive Matrix Factorization (PMF). This study employed the Unmix and PMF model in the source apportionment because these models do not require the external source profiles as inputs.

Visibility is an excellent indicator of air quality. The visual range used to refer to the farthest point that can be seen by the human eye is a primary visibility attribute that can be quantitatively measured (EPA, 1979). Visibility degradation is optically attributed to the scattering and absorption of visible light by both particles and airborne pollutants in the atmosphere (Appel et al., 1985; Latha and Badarinath, 2003). Therefore, changes in visual range can be related to changes in the chemical and physical properties of the atmosphere.

Objectives

The objectives of this study were to evaluate the prescribed burning impacts on air quality at Flint Hills and Kansas City sites; identify the advantages of Unmix and PMF receptor models, and establish a relationship between visibility and $PM_{2.5}$ sources.

1.2 Literature review

During prescribed pasture burning event, measuring emission profiles and $PM_{2.5}$ emission sources directly on site are scarce. In order to address burning impacts for both local and downwind regions, there is a need for knowing the $PM_{2.5}$ emission sources and their contributions. The source apportionment study of multiple locations in Kansas could improve the understanding of the $PM_{2.5}$ origins under rural and urban environments, and further, reveal the source profile of smoke emitted from prescribed burning.

1.2.1 Unmix model applications

The Unmix models have been successfully applied in numerous source apportionment studies, including $PM_{2.5}$ (Anderson et al., 2006; Eatough et al., 2006; Engel-Cox and Weber, 2007; Hu et al., 2006; Ke et al., 2013; Kim et al., 2004; Lang et al., 2015; Lewis et al., 2003; Maykut et al., 2003), secondary pollutants (Anderson et al., 2006), and volatile organic compounds (VOCs) (Ethirajan and Mohan, 2012; Song et al., 2008).

Unmix model assumes that data are linear combinations of an unknown number of sources with unknown chemical composition. For each source, there are samples at the receptors that contain little or no contribution from that source, and these samples produce edges in the measured data. These edges are then created in a multidimensional space. Unmix determines the number of sources and their respective species profiles based on these highly dimensional edges (Anderson et al., 2006; Lewis et al., 2003). The mathematical and geometrical details are presented by Henry (2003).

Maykut et al. (2003) applied the Interagency Monitoring of Protected Visual Environments (IMPROVE) data in the Unmix model and obtained a five-source solution consisting of gasoline, diesel, vegetative burning, fuel oil, soil, and marine sources. A seasonal effect of the vegetative burning and secondary sulfate sources were observed in Unmix derived results. They also suggested that Unmix was able to distinguish diesel emissions from other mobile sources when used temperature-resolved carbon fractions rather than the organic carbon (OC) and elemental carbon (EC) species.

Lewis et al. (2003) derived a five-source solution using Unmix model; the apportioned sources were diesel, vegetative burning, secondary, gasoline, and crustal/soil. This was the first demonstration for an urban area of the capability of the Unmix receptor model. Although species' uncertainty is not required input data, the Unmix model estimates the number of contributing sources and compositions with uncertainties. In identifying $PM_{2.5}$ sources, Lewis et al. (2003) provided a wood burning tracer by using the potassium species without its soil contribution. This tracer element and the amount of OC and EC helped to identify the vegetative burning source from the ambient $PM_{2.5}$.

Mijic et al. (2012) used the Unmix model on PM_{10} pollution with a four-source solution: fossil fuel combustion, traffic exhaust/regional transport from industrial centers, traffic-related particles/site-specific sources and mineral/crustal matter. In their study, the Unmix results were coupled with surface wind direction data to provide identification of the locations of local emission sources affecting a receptor site.

1.2.2 PMF model applications

The PMF model is a newer model than Unmix. Both Unmix and PMF are multivariate models with non-negativity constraints, but they are based on completely different algorithms. After identifying the sources using Unmix, using the PMF model or other individual component analysis to confirm the results is recommended (Eatough et al., 2006).

The PMF model is more complex and time-consuming compare to Unmix (Song et al., 2006a). The PMF model has been used in $PM_{2.5}$, PM_{10}, and VOC studies under different scenarios, (Brown et al., 2015; Eatough et al., 2006; Ke et al., 2013; Kim et al., 2004; Lang et al., 2015; Lee et al., 1999; Paatero and Tapper, 1994; Pandolfi et al., 2011; Pekney et al., 2006a; Pekney et al., 2006b; Rai et al., 2016; Song et al., 2006a).

The PMF model uses alternative least squares to decompose a matrix of speciated data into source profiles and source contribution matrixes. The PMF model accounts for uncertainties in the input data. Therefore, the error estimates for each data point are utilized as point-by-point weights and the inclusion of uncertainty data in the analysis is given lower weights. Moreover, the PMF solution is not as sensitive to the input species. Maykut et al. (2003) suggested the Unmix model solution could be used to guide the choice of the number of sources used in PMF, and the PMF model can guide the choice of species used in Unmix.

Using the PMF model, Maykut et al. (2003) obtained an eight-source solution (gasoline, diesel, vegetative, fuel oil, soil, marine, Na-rich and secondary). Compare to the Unmix model, the PMF is not greatly sensitive to its input species. Therefore, the PMF derived solutions then contain more species then Unmix solutions, and some of these species are considered tracer elements of a certain source. In this case, the PMF result predicts an enrichment of arsenic in the vegetative burning profile, which was not accepted as input species in Unmix. A high correlation coefficient (r=0.84) was later found between Unmix derived primary combustion source (vegetative burning) and arsenic.

1.2.3 Studies focused on the comparison of receptor model results

Applying the same dataset into multiple receptor models is more convincing in model comparison. Song et al. (2006b) conducted source apportionment in PMF using speciated $PM_{2.5}$ data from Beijing; and eight sources were identified: biomass burning, secondary sulfates, secondary nitrates, coal combustion, industry, motor vehicles, road dust, and crustal dust. They reported the improved results based on the original inorganic data from the same set of samples analyzed in the CMB model by Zheng et al. (2005). Maykut et al. (2003) reported that the PMF model was also able to resolve various combustion sources without additional temperature-resolved carbon fractions.

Several studies conducted the source apportionment comparison between Unmix and PMF models (Ethirajan and Mohan, 2012; Kim et al., 2004; Lang et al., 2015; Poirot et al., 2001; Rai et al., 2016). Using multiple receptor models in source apportionment simultaneous is a common agreement in resulting more reliable and interpretable results. However, a drawback of using receptor models was the limitation in quantifying low-strength sources (Lewis et al., 2003; Maykut et al., 2003).

In summary, Unmix and PMF models are currently an efficient way of addressing source apportionment without external source profiles. The potential concerns could remain on result validation and secondary aerosols. The approach of using multiple receptor models can take advantage of the additional resolving power obtained from the different algorithms and may be generally applicable to $PM_{2.5}$ apportionment applications in an area with limited external source profiles. The secondary organic aerosols (SOA) are the major component in $PM_{2.5}$, which cannot be measured directly with its complicated formation mechanism.

1.2.4 Existing visibility impairment studies

Numerous studies have investigated the aerosol influence on visibility impairment (Chan et al., 1999; Zhang et al., 2004). Impairment of visibility is not just an aesthetic problem, it has aroused public attention on air pollution and health concerns (Watson, 2002). The London smog caused by industrial coal combustion and the Los Angeles smog caused by automobile emission combined with photochemical reactions are famous visibility deteriorating events (Brimblecombe, 1981; Tiao et al., 1975). Visibility also affects all forms of traffic, including road, sailing, and aviation safety. An accurate understanding of the visibility impairment is indispensable in public safety and pollutant control strategies, however, the influence of $PM_{2.5}$ sources on visibility was not well understood. Receptor model derived $PM_{2.5}$ sources can provide a more detailed understanding of optical properties of fine particulate matter. To develop a practical control strategy for visibility impairment, both climatological and anthropogenic impacts must be well estimated.

1.3 Methods

1.3.1 Sampling locations and data sources

The two sampling sites in this study were Flint Hills rural site and Kansas City urban site. The Flint Hills site is located near Strong City, KS (38°N, 97°W), with an elevation of 390 m. It is positioned at the center of the Tallgrass Prairie National Preserve, which is favorable for determining fire smoke emissions under all wind directions. The Kansas City monitoring site is positioned at the John F. Kennedy Community Center (JFK Center was renamed Beatrice Lee Community Center in September 2017) in downtown Kansas City (39°N, 94°W), 256 m above sea level. Figure 1 is a satellite image from NASA showing the burning activities in 2014 with the marked sampling locations in this study.

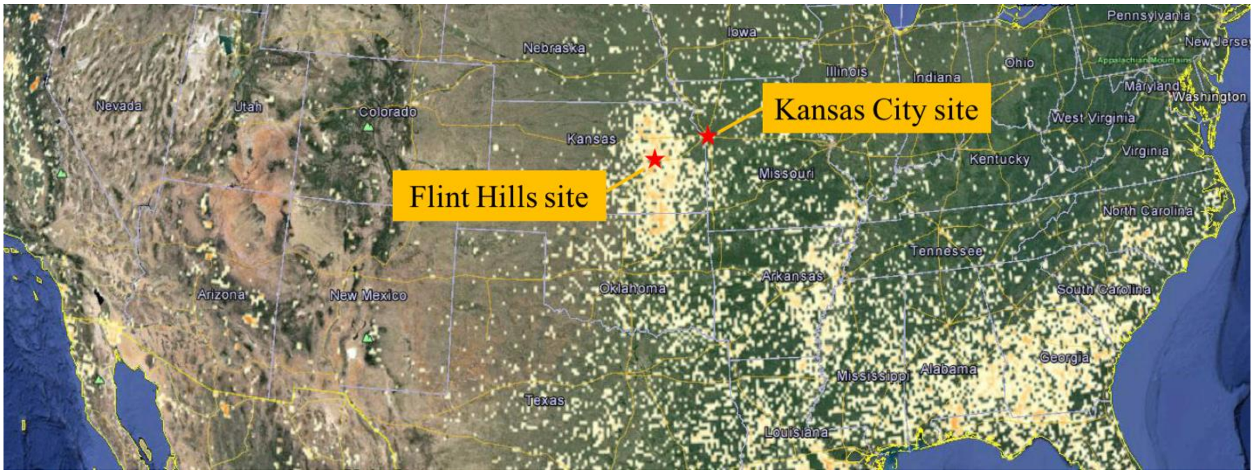

Figure 1 NASA satellite image of burning activities in 2014 and locations of the speciated $PM_{2.5}$ sampling sites

Data acquired for this project includes the speciated $PM_{2.5}$ data (values, uncertainties, and detection limits) and meteorological data (wind direction, wind speed, temperature, relative humidity, visibility) from both sites. The speciated $PM_{2.5}$ data contained the chemical composition of $PM_{2.5}$ in the monitored environment. The Interagency Monitoring of Protected Visual Environments (IMPROVE) sampling network supported the Visibility and Regional Haze Regulation Programs and provided multiple years of quality assured speciated $PM_{2.5}$ data for the Flint Hills sampling site (Solomon et al., 2014). The $PM_{2.5}$ from IMPROVE site was measured by modules with Teflon, nylon and quartz filters. The Chemical Speciation Network (CSN) was housed in the EPA Air Quality System (AQS) database (http://views.cira.colostate.edu/fed/DataWizard), which provided the speciated $PM_{2.5}$ data for Kansas City site. $PM_{2.5}$ was collected on the teflon and nylon filters of the MetOne sampler (Solomon et al., 2014). Both data network can be found on the Federal Land Manager Environmental Database website (http://views.cira.colostate.edu/fed/DataWizard/). At both sites, filters with 24-h duration measurements were collected every three days. A 24-h averaged $PM_{2.5}$ level was recorded as one data point. The Flint Hills site had 1575 valid data points from September 26, 2002 to December 29, 2015, and the Kansas City site had 767 valid data points from June 6, 2001 to October 7, 2009.

The basic meteorological data such as air temperature, relative humidity, precipitation, and solar radiation were from the KSU Mesonet. Stations in Manhattan and Olathe were the closest Mesonet weather stations to $PM_{2.5}$ sampling site and then selected to represent the FH rural and KC urban site. Wind speed, wind direction, and visibility data were provided by the NOAA Surface Data Hourly Global (DS3505) network from the Emporia municipal airport and the Johnson county executive airport, respectively. Note that the wind direction data was calculated using the vector average method from the GSOD hourly wind speed and direction.

1.3.2 Speciated $PM_{2.5}$ data sorting

Both IMPROVE and CSN provided more than 50 speciated $PM_{2.5}$ species, model data preparation was then conducted based on the amount of missing data and minimum detection limit. A species was excluded from the sorted data if that species has more than two-thirds missing data, or data values in this species have more than two-thirds under the minimum detection limit. Missing data in the included species was represented by the missing data symbol “-999”. Data under detection limit in the included species were replaced with a ½ detection limit of this species (Norris et al., 2007). Fine potassium is one of the included $PM_{2.5}$ species. It is mainly emitted from soil dust and biomass burning (Park et al., 2007). To provide a tracer associated with vegetative burning, a calculated parameter non-soil potassium (K_{non}) was introduced. This study used the speciated iron (Fe) concentration as a surrogate for K from the soil to separate the soil K from the total K concentration (Kreidenweis et al., 2001; Ma et al., 2003). The relationship of K_{non} versus Fe was derived from aerosol concentration's scatter plots for both sites (Equation 1):

$$K_{non}=K-0.34\times Fe \qquad \textbf{(1)}$$

where K_{non} is the non-soil potassium, K is the total fine potassium, and Fe is the total iron in the datasets. Meteorological data was then coupled with pre-sorted speciated $PM_{2.5}$ datasets for both sites.

1.3.3 Receptor model implementation

The two receptor models have different principles to select input species. In the Unmix model, users make important decisions on species selection prior to the mostly automated procedure (Lewis et al., 2003). The initiation of Unmix begins with maximizing the number of input species and resultant sources while producing physically realistic and interpretable result (Poirot et al., 2001). The initial input were species with a mean mass concentration greater than 1μg/m^3. Other species in the suggested species list were then tested for Unmix selection by adding in or removing from the selected species in seeking the most suitable solution. Species that can obtain a minimal solution whose diagnostic indicators are acceptable are selected. Diagnostic indicators include R^2 and the signal-to-noise ratio (S/N ratio). A feasible solution of contributing sources should assure at least 80% of the variance of each species could be explained by these sources ($R^2 > 0.8$) and the signal-to-noise ratio greater than 1.5. $PM_{2.5}$ was assigned as the total species. The Unmix model utilizes the self-modeling curve resolution technique to resolve meaningful source factors (Miller et al., 2002). Edge plots are scatter-plots of one species versus another; it is used for identifying species with good edges. Edges that are dependent on many data points rather than a few points will be less likely affected by errors. (Norris et al., 2007) Uncertainties in the solutions of source contributions to $PM_{2.5}$ were estimated by a bootstrap procedure (Efron and Tibshirani, 1993), in which the data are resampled more than 100 times with replacement and the standard deviation of these resampled results give an estimate of the 1-sigma uncertainty.

PMF requires both speciated $PM_{2.5}$ data and their uncertainties. Uncertainties allow each data point to be individually weighted in the PMF solution (Norris et al., 2009). Compared to the Unmix model, the PMF solutions are not as sensitive to the choice of input species (Maykut et al., 2003). First of all, the imported species were categorized into "Bad", "Weak", and "Strong" classes based on their S/N ratio (López et al., 2011). $PM_{2.5}$ was assigned as a total variable, which is default to be "Weak" category. The number of the source in the PMF model was given by the user prior to running the model. The Unmix model has the ability to suggest the solution by self-modeling, which provided the number of sources and source profiles. The number of sources derived from Unmix result was used as a reference to start the PMF modeling. In the PMF model, the solution with the lowest Q (Robust) value was used as the optimal solution for future analysis. The ultimate solution was considered only when the Q(true) is less than 1.5 times of Q (robust), indicating the PMF solution is not influenced by peak events (Gupta et al., 2012).

$PM_{2.5}$ source solutions derived from the Unmix and PMF models from both sites were then compared and analyzed. Radar charts were used to illustrate how source categories identified by the receptor models varied with wind directions.

1.3.4 Visibility measurement and processing method

To evaluate the source-oriented visibility influence, the historical meteorological data and visibility data were employed. Visibility was measured in miles by a forward scatter visibility sensor. Ten miles or greater visibility was recorded as ten miles. The air and dew point temperatures were measured in Fahrenheit by a modern version of the fully automated "HO-83" hygro-thermometer. The hourly RH was calculated from the measured air temperature and dew point temperature using the Clausius-Clapeyron equation. Daily wind direction was determined in vector calculation with hourly wind direction and wind speed. The Tobit analysis in QLIM procedures of SAS (SAS for Windows, version 9.4, SAS Institute, Cary, NC, USA) was used, significant effects were declared at $p<0.05$.

1.3.5 Temporal visibility variation analysis method

Seasonal visibility variation was investigated because the diurnal variation is related to boundary layers, solar radiation, and temperature (Zhao et al., 2013). Seasons were classified by month based on the climate normal in order to find seasonal visibility variation. With January being the coldest month, and July the hottest month in Kansas; winter was to describe December of the previous year, January, and February, and summer includes June, July, and August. Mornings are considered with high RH (Doyle and Dorling, 2002; Ghim et al., 2005) and low mixing heights (United States Bureau of Land Management, 2008). Studies often use winter morning as an observation period since the high RH and low mixing heights condition is enhanced in winter. Afternoon mixing heights are generally higher, especially during summer time due to more heat and less latent heat requirement. A visibility observed during summer afternoon could show the effect of photochemically produced particles (Ghim et al., 2005; Watson, 2002).

1.4 Results and discussion

1.4.1 The Flint Hills rural site

The Unmix model result

The Unmix model resulted in a five-source solution using 10 species ($PM_{2.5}$, aluminum (Al), elemental carbon (EC), organic carbon (OC), iron (Fe), nitrate (NO_3^-), silicon (Si), sulfate (SO_4^{2-}), sulfur (S), and K_{non}) (Liu et al., 2016). The estimated minimum signal-to-noise (S/N) ratio was 6.02, and the $R^2 = 0.91$. Source contribution and composition are shown in Table 1. Table 2 listed the Pearson correlation coefficient of Flint Hills Unmix sources and species that were not selected as the model input but associated with the model result. Monthly source contribution and time series plots are shown in figures 2 and 3.

Table 1 Flint Hills (FH) site Unmix model results-Source contribution and composition (μg/m³)

Source	***Nitrate/agricultural***	***Sulfate/industrial***	***Crustal/soil***	***Smoke***	****SOA***
Code	FH-U1	FH-U2	FH-U3	FH-U4	FH-U5
Contribution	21%	31%	13%	7%	28%
$PM_{2.5}$	1.61	2.31	1	0.49	2.07
OC	0.064	0.03	0.085	0.185	0.519
EC	0.021	0.02	0.005	0.121	0.062
NO_3^-	0.675	0.002	0.027	0.029	0.022
SO_4^-	0.106	0.552	0.16	0.098	0.078
Si	0	0.012	0.112	0.028	0.003
K_{non}	0.002	0.001	0.001	0.044	0.004
Al	0	0	0.054	0.016	0
Fe	0.001	0.003	0.031	0.005	0.001
S	0.029	0.203	0.059	0.037	0.03

*SOA: secondary organic aerosols

FH-U1: Nitrate/Agricultural

The nitrate/agricultural source was identified with the conspicuous agreement with nitrate. This source accounted for 21% of $PM_{2.5}$ mass at the Flint Hills site with a regular seasonal pattern. High loadings were observed in winter months and low loadings found in summer months (Figure 2). Ammonium nitrate is produced by neutralizing nitric acid (HNO_3) with ammonia (NH_3) (EPA, 1995). Kansas nitrate/agricultural source provided sufficient precursor ammonia (NH_3), the ambient nitrate is expected to be fully neutralized ammonium nitrate. Composite source profile estimated the contribution from ammonium nitrate and ammonium sulfate occupied 48% $PM_{2.5}$ in this source. Ammonium nitrate formation is a reversible reaction influenced by ambient temperature. Therefore, the low temperature in winter months favors more particulate ammonium nitrate (Pitchford et al., 2009). In the winter months (December to February), the average monthly temperature is 0°C (NOAA, Strong City, KS), and the nitrate/agricultural source contributed 53% to 56% of ambient $PM_{2.5}$; while from June to September, the average monthly temperature is 23°C and the nitrate/agricultural source contribution is 1.7% to 3.4%. Previous studies have characterized the episodic nitrate pollution in the Midwest U.S (Katzman et al., 2010; Kim et al., 2014; Pitchford et al., 2009). Besides the sufficient agricultural originated NH_3, the secondary nitrate formation is also susceptible to inversions. Winter months with low surface temperatures, low turbulent mixing, and high-pressure systems hasten the stagnant conditions, which is the meteorological driver of high loadings of nitrate/agricultural source during this time.

FH-U2: Sulfate/Industrial

The sulfate/industrial source is the major mass contributor to the ambient $PM_{2.5}$. The high loading of sulfate is a characteristic of this source. In most cases, the sulfate is fully neutralized and in the form of ammonium sulfate. Secondary sulfate in this source may represent origins from coal-fired power plants, vehicle emissions, and other industrial operations. Selenium is believed associated with coal combustion in source apportionment (Pekney et al., 2006b). As seen in Table 2, a 0.6 Pearson correlation found with this source indicating the coal-fired power plant could be a major contributor to the sulfate/industrial source. However, the $PM_{2.5}$ contributed by the coal-fired power plants cannot be recognized as a single source yet in the receptor model; sources like this were called low strength sources. Without other unique tracer elements and lacking featured emission patterns brought difficulties in partitioning sulfate/industrial source into further low strength sources. A periodic pattern with high loadings in summer and low loadings in winter is apparent (figure 2), which is compatible with the effect of photochemical reaction and the presence of oxidants for the secondary sulfate formation. Time series plots have shown a decreasing trend since 2005, which may due to the long-term stringent SO_2 regulation such as the Clean Air Non-road Diesel Rule and the Acid Rain Program for utilities. Studies reported the similar atmospheric sulfate decreasing correspond with controls implemented in the U.S. (Henneman et al., 2015; Hubbell et al., 2010).

Table 2 Pearson correlation coefficient of the Flint Hills Unmix sources and some species.

	FH-U1	FH-U2	FH-U3	FH-U4	FH-U5	C*a*	Cu	Pb	Mn	Se	Ti	Zn
FH-U1	1.00											
FH-U2	-0.06	1.00										
FH-U3	-0.17	-0.13	1.00									
FH-U4	0.03	-0.03	0.00	1.00								
FH-U5	0.03	0.02	-0.05	0.52	1.00							
Ca	-0.11	-0.05	0.50	0.21	0.18	1.00						
Cu	0.07	0.13	0.08	0.49	0.06	0.16	1.00					
Pb	0.36	0.22	-0.03	0.27	0.36	0.13	0.29	1.00				
Mn	-0.12	-0.03	0.86	0.21	0.12	0.73	0.21	0.12	1.00			
Se	0.02	0.62	0.05	0.18	0.33	0.09	0.24	0.38	0.16	1.00		
Ti	-0.16	-0.05	0.97	0.10	-0.01	0.44	0.17	0.02	0.85	0.12	1.00	
Zn	0.43	0.12	-0.06	0.47	0.53	0.19	0.26	0.65	0.16	0.34	0.00	1.00

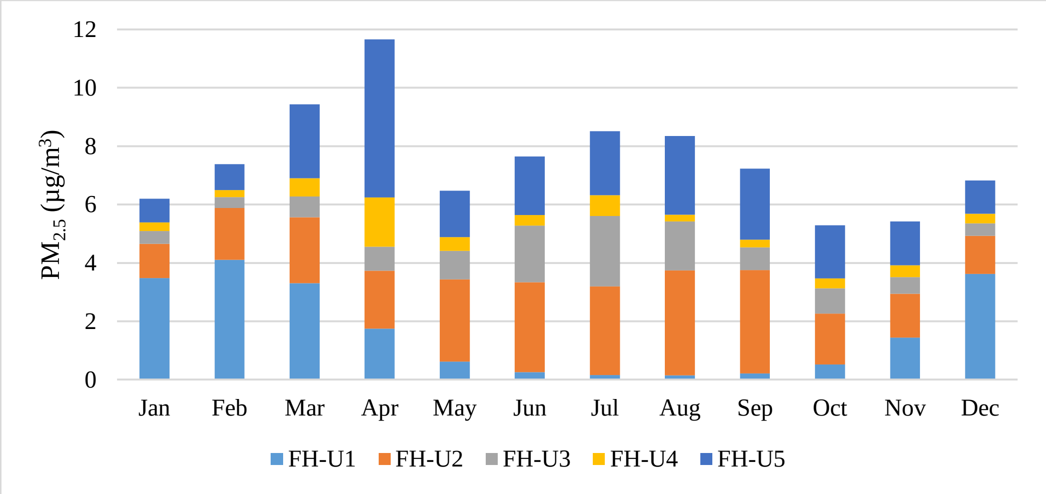

*FH-U1: Nitrate/Agricultural; FU-U2: Sulfate/Industrial; FH-U3: Crustal/Soil, FH-U4: Smoke; FH-U5: SOA

Figure 2 Monthly source contribution from Unmix model result at the Flint Hills site

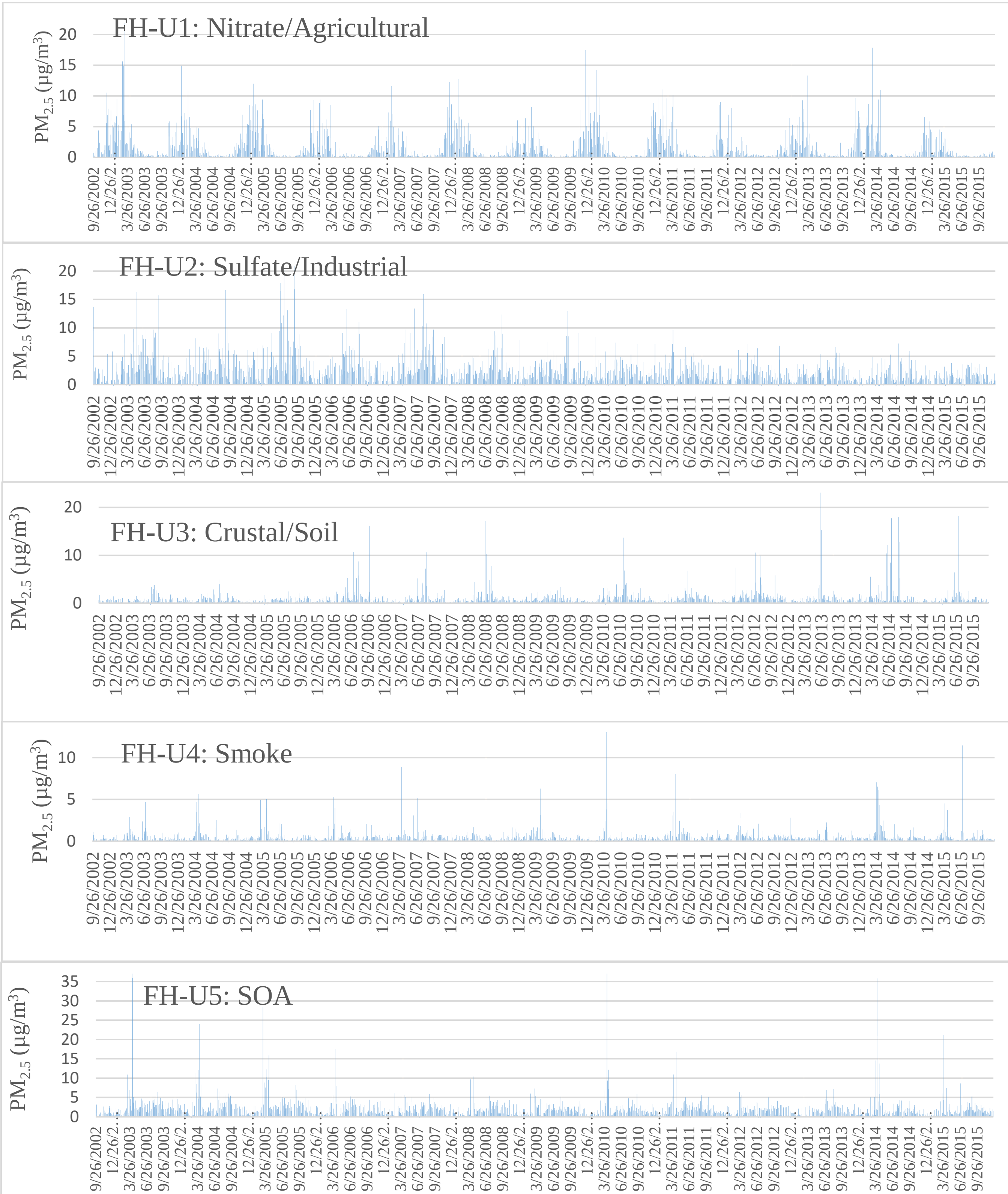

Figure 3 Time series of Flint Hills Unmix source contributions on $PM_{2.5}$ (dates are in m/d/y)

FH-U3: Crustal/soil

The crustal source often consists of oxides of aluminum, silicon, iron, and other metal oxides. Other geological material elements such as Ti, Ca, and Mn also correlated well with this source as shown in table 2, although they were not selected as the input species in the Unmix modeling. High source loadings were observed occasionally in summer with high wind speed. In these days the suspended dust was agitated and enhanced by the wind. Meanwhile, strong wind expedited the dispersion of secondary aerosols, which explains the negative relationship found between crustal/soil source and nitrate/agricultural, sulfate/industrial, secondary organic aerosol (SOA) sources. The crustal/soil source contributed 13% of the total $PM_{2.5}$, which is agreed with reported 5-15% range of a typical geological material contribution in $PM_{2.5}$ (Watson et al., 1994).

FH-U4: Smoke

This category was featured by non-soil potassium since Potassium is a good marker for vegetative burning (Watson et al., 2001), and supported by outstanding contribution in burning season and episodes high EC content. EC is reported to associate with biomass burning (Pekney et al., 2006a), about 53% EC contributed to this source. Smoke source also includes crustal elements of Al, Fe, and Si, indicated partially suspended smoke dust could be crustal/soil originated. The annual average from this source contributes 0.49 $\mu g/m^3$ to ambient $PM_{2.5}$, while in April this contribution reaches the peak monthly-average 1.69 $\mu g/m^3$. Time series also showed the consistent spikes in April, which the intensive prescribed burning usually occurs in the Flint Hills region. Spikes in Aprils are found corresponded with each year's burning area. From 2002 to 2015, an average of 2.1 million acres field was burned each year, while in 2013 only 0.2 million acres were burned due to the unfavorable meteorological conditions. Correspondingly, there are no smoke-originated high loadings of $PM_{2.5}$ observed during the burning season in 2013. The second high loading of this source was observed in July, leading by several extreme events in early

July. The fireworks in July 4th celebration could be the cause for such spikes in this source. Table 3 listed some dates with high smoke source contribution to the ambient $PM_{2.5}$. Moreover, EC is a primary pollutant emitted directly from combustion, while OC has both primary and secondary components. Compare to the OC/EC ratio in FH-U5 (8.4), the smoke source carries a much smaller OC/EC ratio (1.5). All of the above provide evidence for identifying this category as smoke primary aerosols from vegetative burning.

Table 3 Example of early July smoke source contributions to ambient $PM_{2.5}$ (μg/m^3)

Date	FH-U4	$PM_{2.5}$	Percentage
7/5/2008	11.14	12.17	91.48%
7/5/2007	5.13	6.39	80.29%
7/5/2015	11.46	14.65	78.25%
7/5/2011	5.66	9.57	59.16%
7/6/2005	2.02	6.38	31.59%
7/5/2003	4.68	15.03	31.17%

FH-U5: Secondary organic aerosols (SOA)

This category was characterized by the great amount of OC components and lack of tracer elements in classifying specific source. OC is the leading element in mass percentage (25%) compared to other sources, and the OC/EC ratio is 8.4, indicating the secondary aerosol formation in this source. Sulfate is the second mass percentage contributor in this source, it could be from distance sources that allow secondary sulfate formation during transport, such as sulfate/industrial source. The time series plot shows repeated elevations in April, implying the prescribed burning was a major contributor to the SOA. Peak values observed in SOA source did not always occur on the same day with high loading of the smoke source; in some cases, peaks in SOA source were observed a few days after the peak found in the smoke source. The delayed timescales in SOA is likely caused by the different formation pathway with the primary smoke particles (Ng et al., 2006). The SOA source is positively related with the smoke source with a Pearson correlation of 0.52 (Table 2), upholding the precursor contribution from prescribed burning. The ultimate high

SOA was in summer months, could be explained by the seasonal elevation in sulfate/industrial source. The SOA contained in this source was not only from smoke aerosols but also from another source like industrial origin.

The previous study used April and all other months' average contribution in estimating the amount of aerosol contributed by prescribed burning. There are approximately 1.05 µg/m^3 primary aerosols and 4.03 µg/m^3 secondary aerosols, and the secondary aerosol was about four times higher than the primary smoke aerosols, which demonstrated the large impact of rangeland burning on SOA formation (Liu et al., 2016).

The PMF model result

The PMF model in the Flint Hills site resulted in a six-source solution using 14 species ($PM_{2.5}$, Al, calcium (Ca), EC, OC, Cu, Fe, manganese (Mn), nitrate, potassium (K), Si, S, titanium (Ti), and K_{non}). The model result can explain 96% variability of the ambient $PM_{2.5}$ data. Source contribution and composition are shown in table 4.

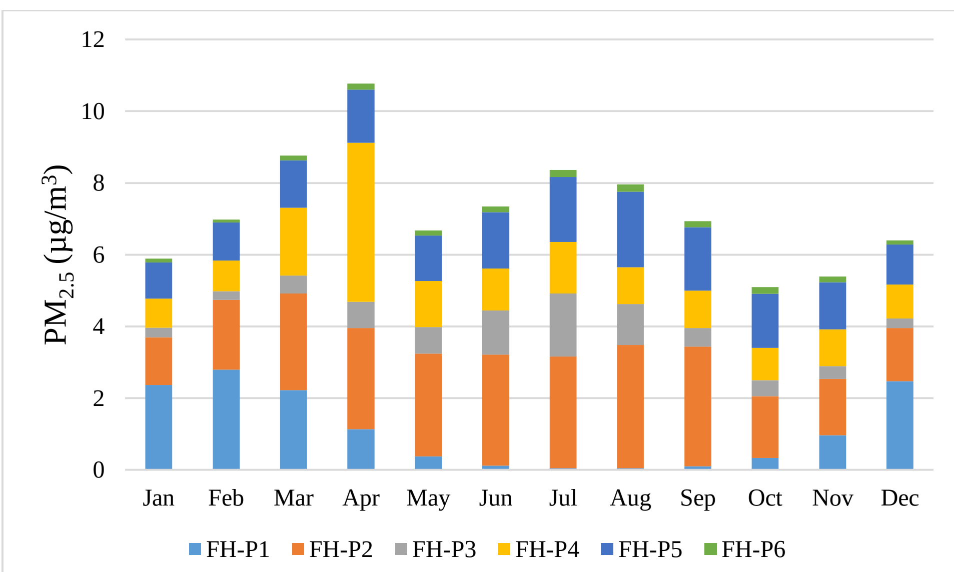

Figure 4 Monthly average source contribution from the PMF model result at the Flint Hills site

Table 4 The FlintHills site PMF model results- Source contribution and composition (μg/m^3)

Source	*Nitrate /agricultural*	*Sulfate /industrial*	*Crustal /soil*	*Smoke*	*Traffic /SOA**	*Ca*
Code	FH-P1	FH-P2	FH-P3	FH-P4	FH-P5	FH-P6
Contribution	15%	34%	10%	19%	20%	2%
$PM_{2.5}$	1.060	2.440	0.680	1.380	1.450	0.150
OC	0.000	0.159	0.054	0.607	0.388	0.000
EC	0.013	0.038	0.000	0.097	0.085	0.000
NO_3^-	1.042	0.022	0.034	0.052	0.027	0.000
SO_4^-	0.086	1.425	0.082	0.000	0.204	0.000
Si	0.000	0.019	0.113	0.003	0.000	0.026
K_{non}	0.001	0.000	0.000	0.027	0.000	0.003
Ca	0.000	0.000	0.005	0.000	0.017	0.067
Al	0.000	0.002	0.041	0.003	0.004	0.004
Cu	0.000	0.000	0.000	0.000	0.000	0.000
Fe	0.000	0.000	0.027	0.000	0.014	0.002
Mn	0.000	0.000	0.000	0.000	0.000	0.000
K	0.001	0.000	0.010	0.027	0.005	0.005
Ti	0.000	0.000	0.002	0.000	0.001	0.000

*SOA: secondary organic aerosols

Table 5 Pearson correlation coefficient matrix of the Flint Hills PMF sources and some species.

	FH-P1	FH-P2	FH-P3	FH-P4	FH-P5	FH-P6	Pb	Ni	Se	Zn
FH-P1	1.00									
FH-P2	0.02	1.00								
FH-P3	-0.19	0.02	1.00							
FH-P4	0.10	0.22	0.02	1.00						
FH-P5	-0.04	0.18	0.06	0.19	1.00					
FH-P6	-0.16	-0.08	0.39	0.11	0.51	1.00				
Pb	0.36	0.30	-0.02	0.39	0.29	0.10	1.00			
Se	0.00	0.66	0.11	0.29	0.33	0.05	0.38	0.00	1.00	
Zn	0.43	0.23	-0.04	0.57	0.36	0.17	0.65	-0.01	0.34	1.00

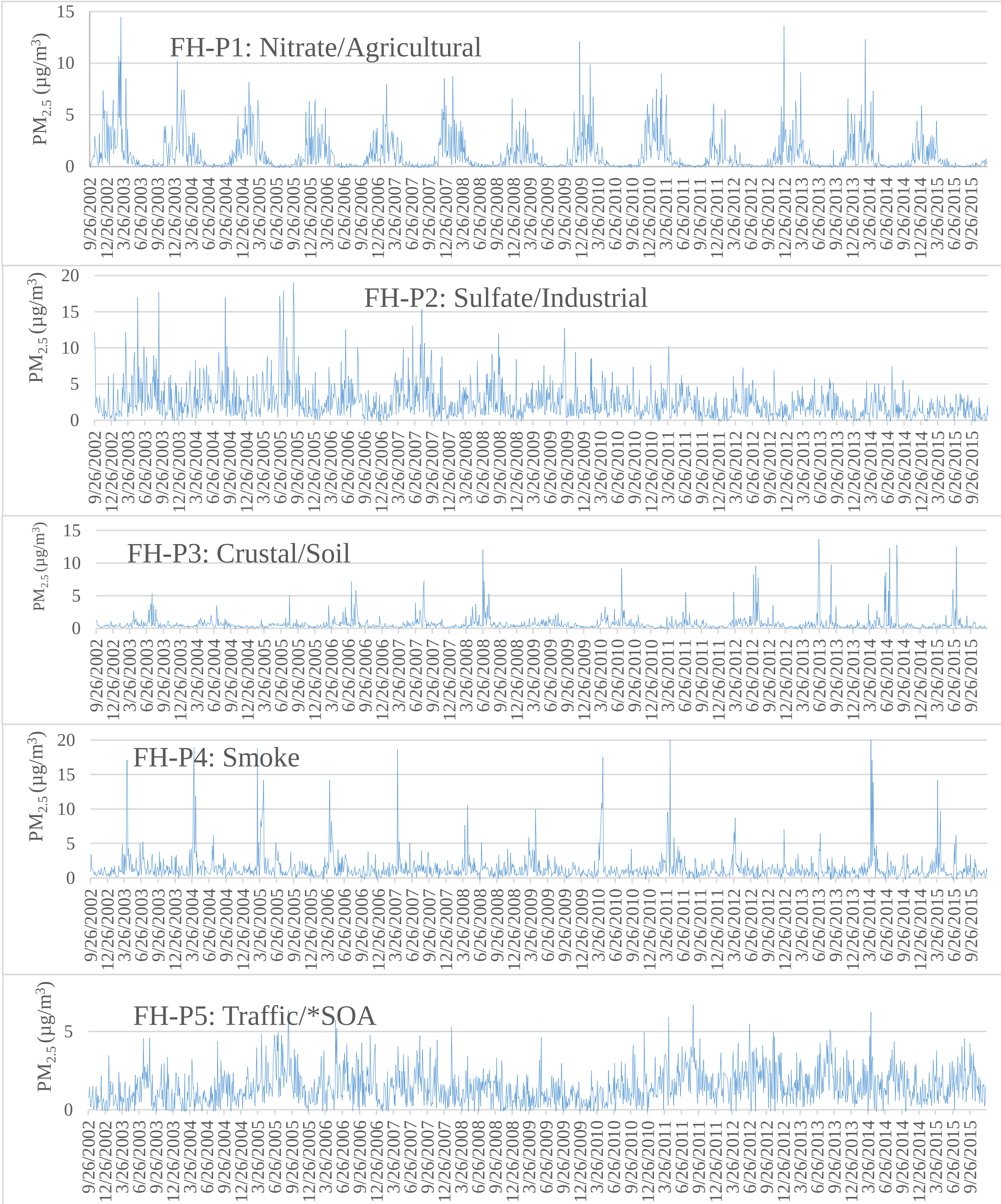

*SOA: secondary organic aerosols

Figure 5 Time series of the Flint Hills PMF source contributions on $PM_{2.5}$ (dates are in m/d/y)

FH-P1: Nitrate/Agricultural

Nitrate/agricultural source in PMF result at Flint Hills site was also identified by nitrate (1.04 μg/m^3). This source accounted for 15% of $PM_{2.5}$ mass with an identical seasonal pattern as in Unmix result. As discussed in FH-U1, secondary nitrate formation in winter months was enhanced by meteorological condition, as well as longer night time (Alexander et al., 2009; Stanier et al., 2012). The FH-P1 and FH-U1 agree well on this source with an R^2=0.99 (as in figure 8), the difference is the absolute value of nitrate is higher in the FH-P1 (1.04 μg/m^3) compare to FH-U1 (0.68 μg/m^3).

FH-P2: Sulfate/Industrial

As the leading contributor to the ambient $PM_{2.5}$, the sulfate/industrial source is featured with high loadings of sulfate. This source accounted for 34% (2.44 μg/m^3) mass percentage of ambient $PM_{2.5}$, with 1.43 μg/m^3 was devoted by sulfate. This source also displays high loadings in warmer months as in FH-U2. Although Selenium (Se) was not selected species in PMF input data, a positive correlation with Se was found with a 0.7 Pearson correlation coefficient (Table 5), upholding the contribution from coal-fired power plants to this source (Khodeir et al., 2012). Time series plot shows a decreasing trend since 2005, possibly associated with regulation in stringent SO_2 emission. The FH-U2 and FH-P2 source contributions agreed well with R^2=0.93 (Figure 8).

FH-P3: Crustal/soil

The crustal/soil source was characterized by geological material elements. The PMF model included more geological elements such as Ca, K, and Ti compare to the Unmix model. Crustal/soil source appeared an elevation in July which agreed with FH-U3. Source contribution is harmonized with an R^2=0.96 between FH-U3 and FH-P3.

FH-P4: Smoke

The smoke source was identified by K_{non} in the PMF as well. Carbonaceous species (EC and OC) are the dominant $PM_{2.5}$ component in this source, occupied 51% mass fraction. Si and Al were also a presence in this source, likely due to smoke dust from the soil. The annual average from this source contributes 1.4 $\mu g/m^3$ to ambient $PM_{2.5}$, while the peak month contributed 4.43 $\mu g/m^3$ $PM_{2.5}$ in April. In April, the FH-P4 source category had the $PM_{2.5}$ contribution about 2.6 times than FH-U4 (1.69 $\mu g/m^3$). The OC/EC ratio in annual contribution from FH-P4 (6.3) is also more than 4 times higher than FH-U4 category (1.5). It is believed that FH-P4 source category included both primary and secondary smoke aerosols.

FH-P5: Traffic/SOA

This category was identified by both mass fraction of nitrate and sulfate, and OC/EC ratio. The OC/EC ratio in the FH-P5 source was 4.6, which was the second high category in the PMF model derived sources. These indicated the presence of SOA. The amount of EC in this group is probably from tailpipe exhaust of motor vehicles. The presence of Ti, Fe, Si, and Ca were implying gasoline and diesel profile (Lewtas et al., 2002). Typical crustal elements could also suggest its soil originated peculiarity as found in road dust sources in another study (Song et al., 2006b). The lack of K_{non} in FH-P5 eliminate the root in smoke, and then it was considered as SOA from non-smoke sources. Accounting for soil and road dust related features, this source category was labeled as traffic/SOA. A positive relationship between FU-P5 and FH-P6 was revealed with a Pearson correlation coefficient of 0.5, possibly due to suspended road dust (Table 5).

By comparing smoke related source from the two receptor models, the FH-U4 was composed of mainly primary aerosols from smoke, while FH-U5 possibly contained SOA from both smoke and other sources. FH-P4 likely includes both primary and secondary smoke originate aerosols, and FH-P5 was presumably contained SOA from non-smoke sources such as engine combustion, mobile, etc. To embody the differences between model results and to demonstrate the previous assumptions, a comparison of smoke-related categories is illustrated in figure 6 on a monthly basis. The FH-P4 level was about 2 to 4.5 times than FH-U4, and the combined level of FH-U4 and FH-U5 was continuously higher than FH-P4. It has confirmed the prior assumption of different SOA allocation between categories in different models. The smoke aerosols including primary and secondary aerosols at the Flint Hills site could be estimated as U4+U5, which carries a high regression coefficient (R^2 = 0.92) with PMF resolved smoke category (P4). When the intensive prescribed burning taken place in April months, the primary $PM_{2.5}$ emitted by prescribed burning can be estimated as 1.69 $\mu g/m^3$ (in FH-U4), and the total $PM_{2.5}$ from burning smoke can be estimated as 4.43 $\mu g/m^3$ (in FH-P4). The approximate amount of SOA from prescribed burning was computed as 2.74 $\mu g/m^3$ (FH-P4 subtract FH-U4), which occupied 62% of the entire smoke source aerosols. Figure 6 also indicated a seasonal elevation in $PM_{2.5}$ in July and August, possibly associated with open burning in the summer, such as campfires.

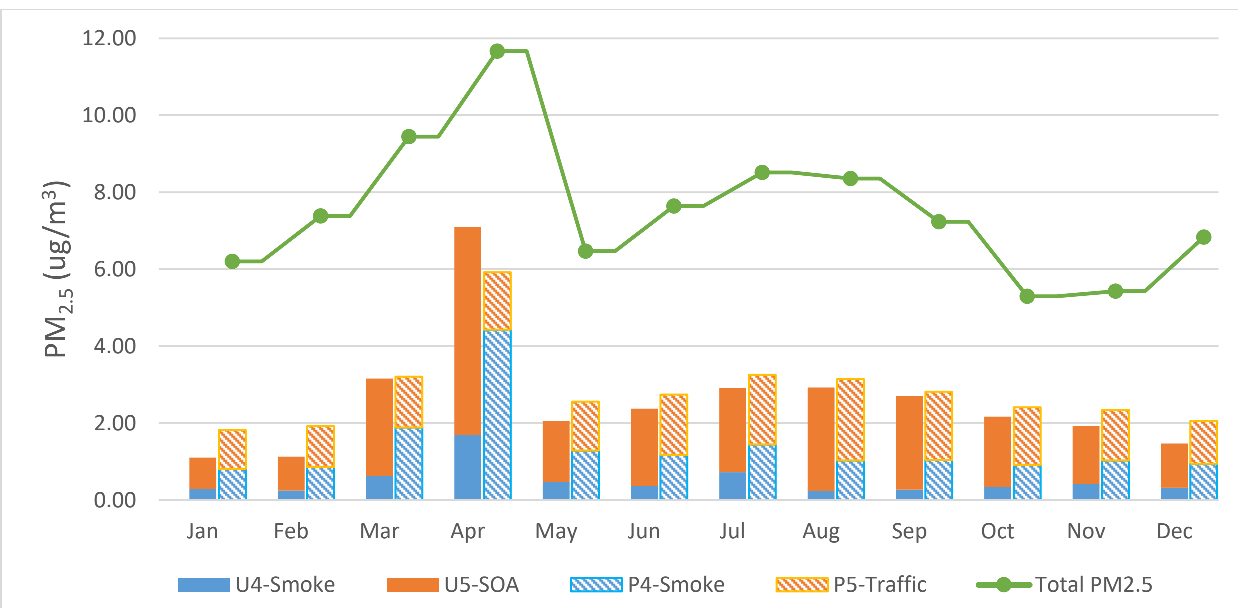

Figure 6 Monthly-averaged contributions of smoke-related sources from both models at the Flint Hills site

Using both model results, the ratio between FH-P4 and FH-U4 was introduced as $PM_{2.5}$ expansion in addition to the primary aerosols in smoke, namely P4/U4 ratio. Figure 7 shows the monthly P4/U4 ratio at the Flint Hills site.

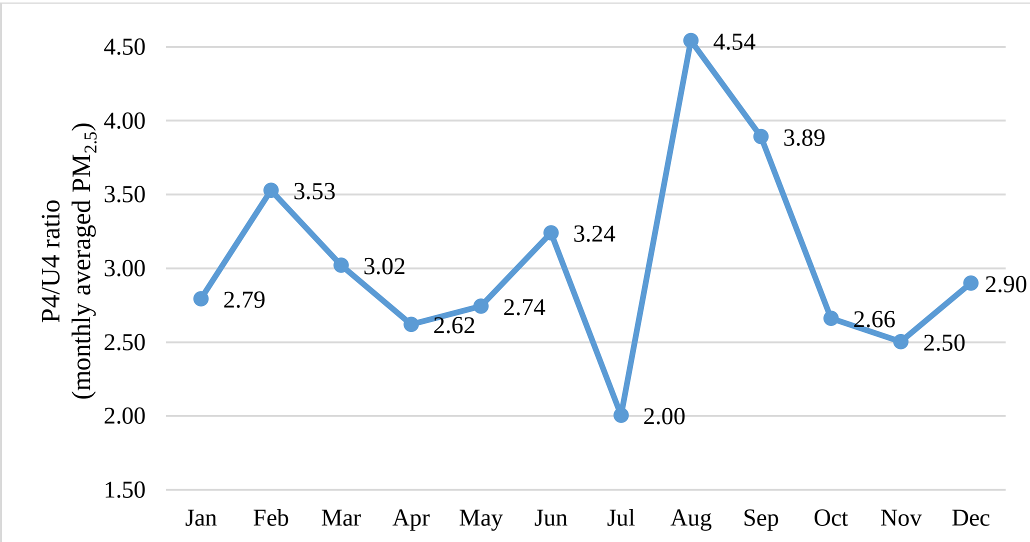

Figure 7 Monthly P4/U4 ratio at the Flint Hills site

A previous study (Liu et al., 2016) has estimated that the contribution of secondary smoke aerosol was about four times higher than the primary smoke aerosols, which demonstrated the large impact of rangeland burning on SOA formation. The P4/U4 ratio shown in the figure has improved the $PM_{2.5}$ expansion in addition to the primary aerosols from prescribed burning. The SOA is about 2.6 times higher than the primary aerosols during the burning season in the month of April. The minimum value of P4/U4 at the Flint Hills site was observed in July, where the P4/U4 ratio is 2. It is reasonable to assume the smoke originated sources in this month carried relatively high primary aerosols, such as campfires. As concluded by other researches (Huang et al., 2016; Wang et al., 2016), the elevation of the P4/U4 ratio also found in warmer months when the atmospheric photochemical reaction is more intensive, as seen in August from figure 7.

FH-P6: Ca dominated source

This source was only categorized in the PMF model at the Flint Hills site, with a high loading of calcium. Ca (0.067 μg/m^3) was the leading contributor to this source, occupied 45% mass fraction of this category. The crustal properties were expressed with a moderate positive correlation (Pearson correlation coefficient = 0.4) between FH-P6 and FH-P3. Across model results, the crustal-related categories of Unmix model (i.e., FH-U3) and PMF model (i.e., the sum of FH-P3 and FH-P6) have a high agreement with the R^2=0.96. A positive correlation between FH-P6 and FH-U5 (SOA source from Unmix model) was also noticed with a Pearson correlation of 0.5. The monthly concentration of Ca dominated source was found slightly higher in warmer months, but no apparent seasonal pattern was observed. After all, the Ca dominated source only has limited impacts to the ambient $PM_{2.5}$, due to its small contribution.

Comparison of the Unmix and PMF modeling results at the Flint Hills site

In summary, the Unmix and PMF models resolved a different number of sources at the Flint Hills site, with similar contributions in the nitrate/agricultural, sulfate/industrial, and crustal/soil source categories. The different number of sources was because the different interpretation of primary and secondary smoke originated $PM_{2.5}$.

In the nitrate/agricultural, sulfate/ industrial and crustal/soil categories, the Unmix and PMF modeling results were in good agreement. Modeling results from the sulfate/industrial source were in high agreement, while $PM_{2.5}$ level from the nitrate/agricultural and crustal/soil source in the Unmix was slightly higher than that in the PMF model result (Figure 8). This could be explained by the source profile of FH-P5 (Traffic/SOA), which was featured by high loadings of nitrate, sulfate, OC, and EC. It is reasonable to assume that the FH-P5 included SOA from agricultural and industrial origins. The smoke category has wider dispersed distribution and presented a higher loading in the PMF result which enclosed both primary and secondary burning related aerosols under the smoke source.

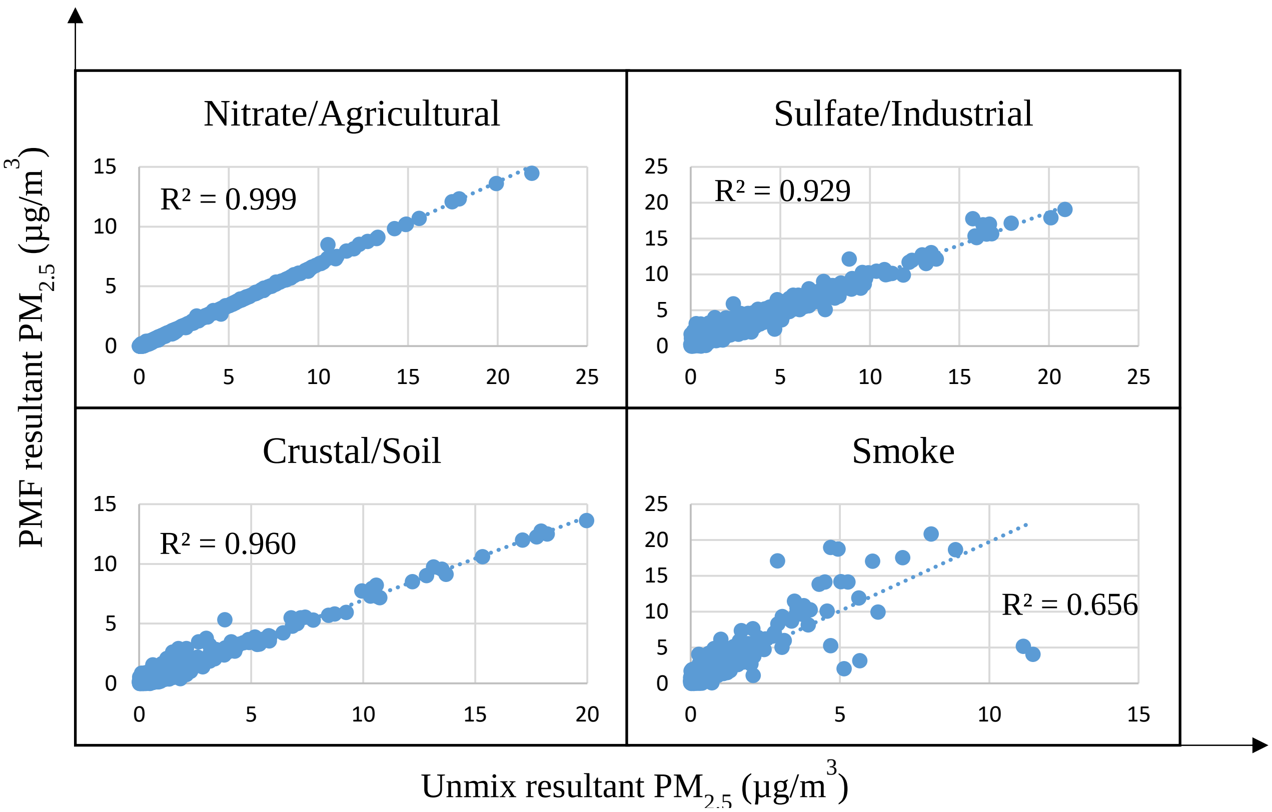

Figure 8 Comparison of the Unmix and PMF results at the Flint Hills site

To further analyze the secondary organic aerosols from the different model derived sources, EC tracer method was introduced. The EC is exclusively associated with primary emission, while OC can be from primary emissions and be formed through secondary pathways. As listed in Equation 2, Turpin and Huntzicker (1995) employed EC as the tracer of primary OC (POC), and used primary OC/EC ratio as a reference; then estimated the amount of secondary OC (SOC):

$$POC=(OC/EC)_{pri} \times EC$$
$$SOC= OC_{total} - (OC/EC)_{pri} \times EC \quad \textbf{(2)}$$

The $(OC/EC)_{pri}$ is the reference OC/EC ratio in primary aerosols. In the current study, receptor models indicated FH-U4 is a primary smoke source in FH site. The $(OC/EC)_{pri}$ =1.5 is then adopted from FH=U4 for Flint Hills site. The computed POC and SOC are 0.927 μg/m^3 and 2.496 μg/m^3 for FH site in burning season, respectively. It is saying the burning originated secondary aerosol is about 2.7 times than the primary aerosols. The burning related source profiles from both receptor models also provided a similar outcome. Using OC/EC ratios from FH-U4 (Smoke), FH-U5 (SOA), and FH-P4 (Smoke) in April, the estimated ratio of burning related secondary aerosols over primary aerosols is 2.3. These findings agreed well with the previous study (Liu et al., 2016), where the smoke source secondary aerosols were three times than the primary aerosols in the burning season.

1.4.2 The Kansas City urban site

The Unmix model result

The Unmix model at the Kansas City site resulted in a seven-source solution with 12 species ($PM_{2.5}$, Al, NH_4^+, EC, OC, Cu, Fe, Mn, nitrate, Si, sulfate, and K_{non}). The estimated minimum S/N ratio was 2.01, and R^2=0.92. Source contribution and composition are shown in Table 6. Table 7 listed the Pearson correlation coefficient of Kansas City Unmix sources and some species that were not included in the Unmix input. Figures 9 and 10 show the monthly averaged source contribution and time series plot of model-derived sources.

KC-U1: Nitrate/ Agricultural

The nitrate/agricultural source was featured by nitrate. This source contributed 25% mass to the ambient $PM_{2.5}$ slightly more than it at the Flint Hills site, but the absolute $PM_{2.5}$ level was more than two times as at the Flint Hills site. Approximately 0.52 μg/m^3 nitrate and 0.19 μg/m^3 ammonium in this source occupied 20% mass percentage. In the role of agriculture, ammonium and ammonium nitrate are an important source of nitrogen in the soil and contribute to plant growth. The nitrate and ammonium species has a similar seasonal variation and are well correlated (Pearson coefficient=0.72). Higher $PM_{2.5}$ were recorded in winter months and lower in summer months because the ammonium nitrate evaporates at a warmer temperature. Studies also pointed out the reduction in NO_x emissions would have limited effects on the production of ammonium nitrate due to the chemical mechanism equilibriums that result information (Lawson, 1998). The OC/EC ratio was 15 in this source, upholding the presence of secondary ammonium nitrate.

Table 6 The Kansas City site Unmix model results-Source contribution and composition (μg/m^3)

Source	Nitrate /agricultural	Sulfate /industrial	Crustal /soil	Smoke	Traffic /SOA*	HDDV**	Cu
Code	**KC-U1**	**KC-U2**	**KC-U3**	**KC-U4**	**KC-U5**	**KC-U6**	**KC-U7**
Contribution	**25%**	**34%**	**3%**	**9%**	**22%**	**3%**	**4%**
$PM_{2.5}$	3.540	4.810	0.420	1.260	3.100	0.464	0.575
Al	0.001	0.000	0.083	0.000	0.000	0.000	0.001
NH_4^+	0.190	0.137	0.060	0.004	0.000	0.000	0.030
EC	0.008	0.014	0.000	0.000	0.131	0.078	0.185
OC	0.128	0.214	0.000	0.303	0.858	0.714	0.576
Cu	0.000	0.000	0.000	0.000	0.000	0.000	0.018
Fe	0.000	0.002	0.035	0.000	0.009	0.052	0.018
Mn	0.000	0.000	0.000	0.000	0.000	0.006	0.000
NO_3	0.522	0.010	0.000	0.020	0.019	0.003	0.019
Si	0.000	0.003	0.138	0.000	0.012	0.019	0.003
SO_4	0.121	0.391	0.349	0.077	0.007	0.032	0.097
K_{non}	0.001	0.000	0.010	0.070	0.001	0.000	0.005

*SOA: secondary organic aerosols   **HDDV: heavy-duty diesel vehicle

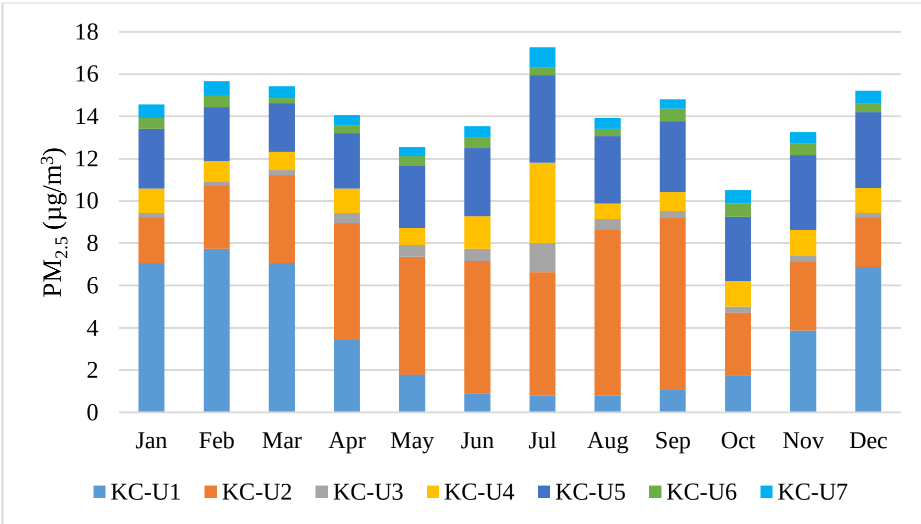

Figure 9 Monthly source contribution from the Unmix model result at the Kansas City site

Table 7 Pearson correlation coefficient matrix of the Kansas City Unmix sources and some species.

	KC-U1	KC-U2	KC-U3	KC-U4	KC-U5	KC-U6	KC-U7	Ca	Pb	K	Se	Ti	Zn
KC-U1	1.00												
KC-U2	-0.15	1.00											
KC-U3	-0.11	-0.11	1.00										
KC-U4	-0.05	-0.06	0.11	1.00									
KC-U5	-0.05	-0.15	0.14	0.00	1.00								
KC-U6	-0.01	-0.11	0.05	0.02	0.07	1.00							
KC-U7	0.04	-0.08	0.05	0.29	-0.08	0.10	1.00						
Ca	-0.15	0.03	0.34	0.06	0.46	0.35	0.21	1.00					
Pb	0.12	-0.09	-0.01	0.10	0.22	0.17	0.23	0.14	1.00				
K	-0.03	-0.08	0.22	0.99	0.06	0.11	0.34	0.16	0.14	1.00			
Se	0.04	0.19	0.06	0.02	-0.01	-0.01	-0.03	0.03	-0.01	0.02	1.00		
Ti	-0.04	0.03	0.66	0.12	0.25	0.11	0.07	0.44	0.05	0.22	0.07	1.00	
Zn	0.14	-0.11	-0.06	0.02	0.41	0.38	0.23	0.22	0.54	0.07	-0.05	0.03	1.00

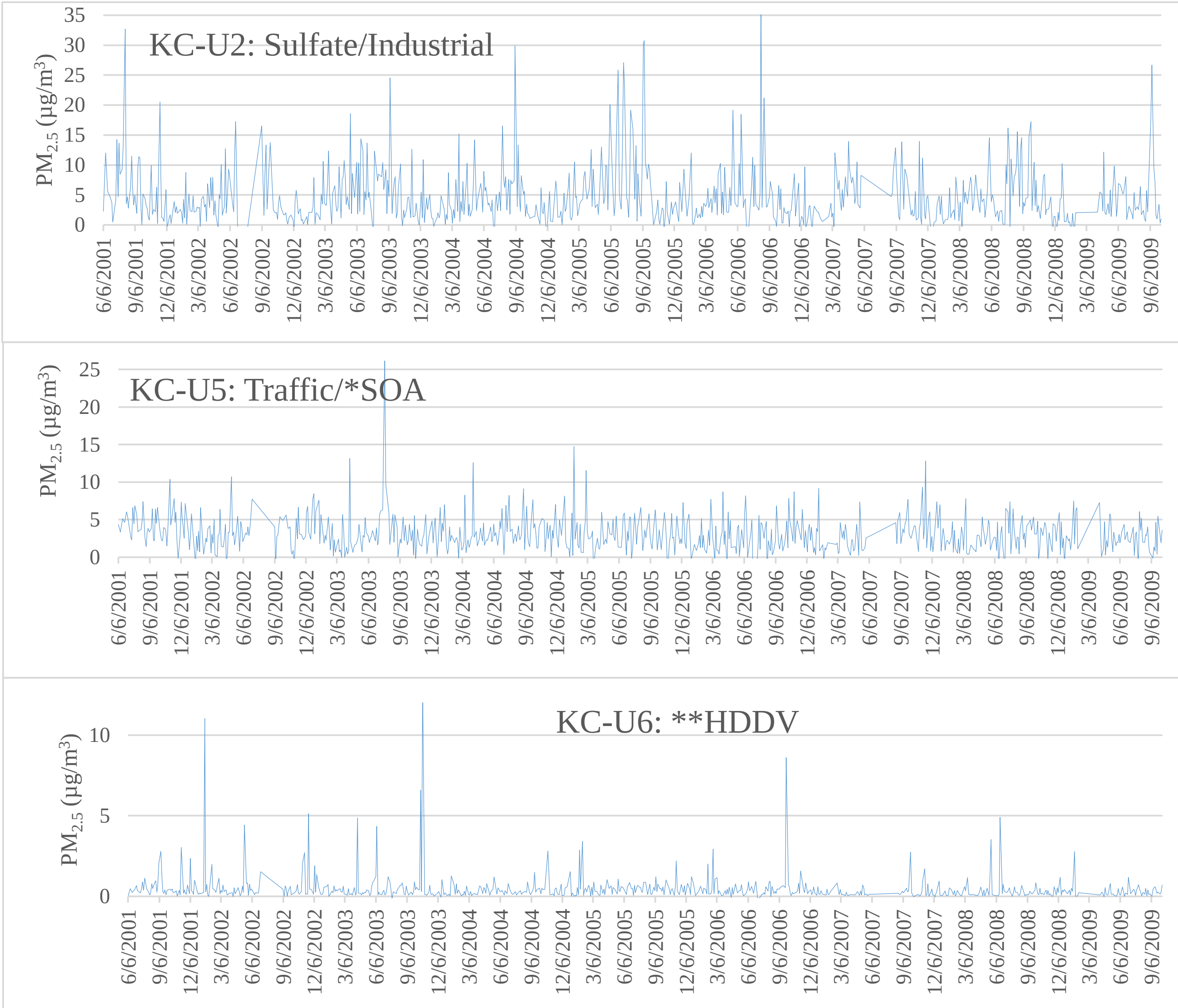

*SOA: secondary organic aerosols **HDDV: heavy-duty diesel vehicle

Figure 10 Time series plots of selected Kansas City Unmix source contributions on $PM_{2.5}$ (dates are in m/d/y)

KC-U2: Sulfate/ Industrial

Sulfate was used to trace industrial source, which is the leading contributor (0.39 µg/m^3, 34%) to ambient $PM_{2.5}$. OC is the second leading contributor in this source, and the OC/EC ratio was 16, which is supporting the presence of the secondary aerosol formation. The average monthly sulfate/industrial level is 4.75 µg/m^3; the highest value was recorded in warmer months especially in August (7.8 µg/m^3) and September (8.1 µg/m^3), it is almost double strength than it in winter months (October to January). The time series indicated a decreasing tendency since 2005, corresponding with the stringent SO_2 regulations. Although sulfate/industrial source contributed a similar mass percentage to total $PM_{2.5}$ as at the Flint Hills site, the absolute value of $PM_{2.5}$ level doubled in Kansas City site; likely due to more anthropogenic emissions in the urban area.

KC-U3: Crustal/ Soil

This crustal source was featured by geological elements such as Al, Fe, and Si. 81% (0.14 $\mu g/m^3$) Si was contributed to this source. Table 7 indicated a positive correlation between elements Ca (Pearson R=0.34), Ti (Pearson R=0.66) and this source. OC and EC were absent, while sulfate occupied 83% mass fraction in this source. The monthly contribution from crustal/soil is about 0.43 $\mu g/m^3$, a remarkable elevation was observed in July with 1.38 $\mu g/m^3$ level of $PM_{2.5}$. Wind-blown soil crust and road dust could be one of the reasons. Secondary sulfate is developed via the chemical reaction of ozone and organic gases, which could be enhanced by high temperature in summer. Moreover, a small portion of ammonium was observed in the crustal/soil source along with sulfate, which could also be explained by gypsum materials.

KC-U4: Smoke

Smoke was traced by K_{non} at the Kansas City site, 78% (0.07 $\mu g/m^3$) K_{non} contributed to this source. The monthly averaged level is 1.29 $\mu g/m^3$, annually contributed 9% to the ambient $PM_{2.5}$. The major contributors are ammonium nitrate and ammonium sulfate (NH_4^+, NO_3^-, and SO_4^-). OC is a leading donor in this source, 0.3 $\mu g/m^3$ OC occupied 24% $PM_{2.5}$ mass fraction, endorsing the composition of secondary aerosols. Monthly average $PM_{2.5}$ showed a significant elevation in July. The absolute $PM_{2.5}$ level was 3.78 $\mu g/m^3$ in July, almost three times than the annual averaged level. Time series plot laid out several data points with $PM_{2.5}$ higher than 10 $\mu g/m^3$, and all excess dates were around 4th of July (June 30th, 2001; July 2nd, 2003; July 5th, 2004; July 3rd, 2005; July

6th, 2005; July 4th, 2006; and July 5th, 2008). Therefore, the 4th of July celebration could be a major contribution to this source. Unlike the smoke source in Flint Hills site, no significant peak was observed in burning season at Kansas City site.

KC-U5 Traffic/SOA

A notable high OC/EC ratio (OC/EC=6.5) of this source stood out along with a major mass fraction (32%) of the carbonaceous species. Si, Fe, and Cu were also included in this source, unveiling the characteristic of fugitive dust, such as unpaved road, traffic suspended dust, and wind erosion from bare soil. A high positive correlation with Ca and Zn was found, with a Pearson correlation coefficient of 0.46 and 0.41 respectively; Pb carries a 0.22 Pearson coefficient with this source. As mentioned in the previous record, Zn could be emitted from lubricant oil, brake linings, and tires, which makes it an indicator of motor vehicle exhaust in the source apportionment; Pb and Zn elements are found in gasoline profile; Fe, Zn, Si, and Ca are found in diesel profile (Lewtas et al., 2002). No obvious seasonal pattern was demonstrated in this source, however, the highest loading month was July (4.12 μg/m^3), while the monthly average was 3.10 μg/m^3.

KC-U6: Heavy-duty Diesel Vehicle (HDDV)

This source is the second small contributor to the ambient $PM_{2.5}$, annually contributed 3% mass percentage. The OC/EC ratio is 9.15 in this source, even higher than that in KC-U5. The slightly higher EC/OC ratio may be due to the influence of diesel engine emissions (Hu et al., 2006). This category also positively related to Ca and Zn with 0.35 and 0.38 Pearson correlation coefficient, upholding the diesel profile. Seasonal variation was not disciplinary from this source, contrarily it had a relative sustainable contribution to ambient $PM_{2.5}$ through sampling years. The Fairfax Traffic way is located about two miles east of the JFK Center sampling site, this train traffic way was presumably the main contributor to the HDDV source category.

KC-U7: Cu dominated

Copper was the leading species in this source, with a 4% contribution to ambient $PM_{2.5}$. The inclusion of OC, EC, ammonium, nitrate, and sulfate demonstrated the secondary feature of this source. Monthly $PM_{2.5}$ elevated in July to about 60% compared to the average, and this source also carried a 0.3 Pearson correlation coefficient with the smoke source (KC-U4).

The PMF model result

The PMF model at the Kansas City site derived a seven-source solution with 15 species ($PM_{2.5}$, Al, NH_4^+, Ca, EC, OC, Cu, Fe, Mn, nitrate, potassium (K), Si, sulfate, zinc (Zn), and K_{non}). The model result can explain 90% variability of the ambient $PM_{2.5}$ data. Table 8 shows the source contribution and composition from the PMF model in Kansas City site. Figure 11 shows the monthly source contribution from the PMF model result at the Kansas City site.

Table 8 The Kansas City PMF results - Source contribution and composition (μg/m³))

Source	Nitrate /Agricultural	Sulfate /Industrial	Crustal /Soil	Smoke	Traffic /SOA*	**HDDV	Cu
Code	**KC-P1**	**KC-P2**	**KC-P3**	**KC-P4**	**KC-P5**	**KC-P6**	**KC-P7**
Contribution	15%	32%	9%	9%	25%	9%	1%
$PM_{2.5}$	2.010	4.370	1.220	1.160	3.330	1.240	0.130
OC	0.110	0.716	0.409	0.439	2.180	0.874	0.054
EC	0.008	0.068	0.020	0.012	0.302	0.118	0.045
NO_3	1.562	0.000	0.060	0.000	0.338	0.000	0.000
SO_4	0.059	1.996	0.161	0.095	0.340	0.000	0.000
Si	0.004	0.000	0.091	0.002	0.000	0.010	0.000
K_{non}	0.001	0.004	0.005	0.089	0.000	0.001	0.000
Ca	0.002	0.000	0.020	0.002	0.007	0.074	0.000
Al	0.001	0.000	0.016	0.001	0.000	0.000	0.002
NH_4	0.495	0.707	0.042	0.000	0.000	0.037	0.014
Cu	0.000	0.000	0.000	0.000	0.000	0.000	0.009
Fe	0.000	0.004	0.016	0.000	0.023	0.021	0.003
Mn	0.000	0.000	0.000	0.000	0.001	0.001	0.000
K	0.001	0.004	0.012	0.088	0.013	0.008	0.001
Zn	0.001	0.001	0.000	0.000	0.005	0.002	0.000

*SOA: secondary organic aerosols **HDDV: heavy-duty diesel vehicle

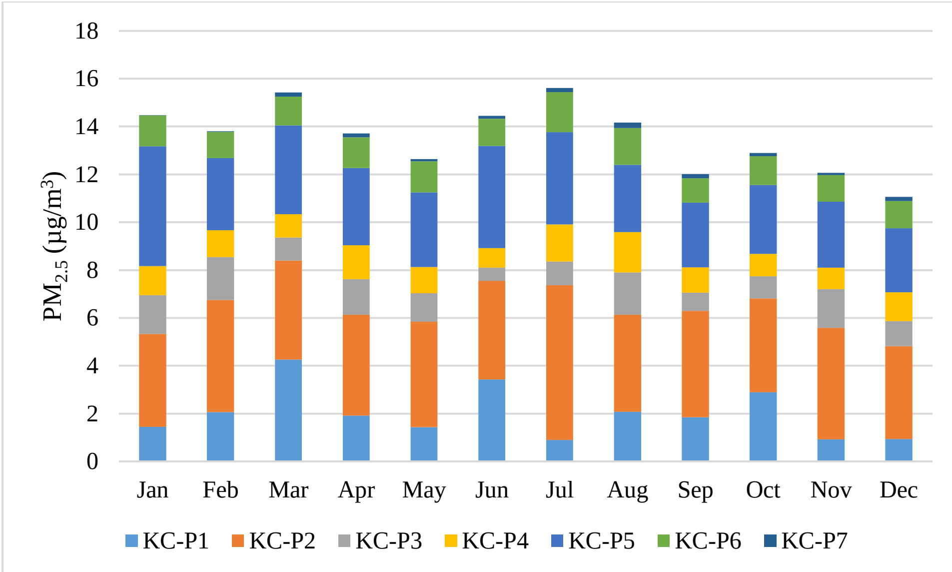

Figure 11 Monthly source contribution from the PMF model result at the Kansas City site

KC-P1: Nitrate/Agricultural

The nitrate/agricultural source contributed 15% mass percentage of ambient $PM_{2.5}$ and was identified by high loadings of nitrate. About 1.56 µg/m^3 nitrate contributed to this source and occupied 77% mass fraction. Regular elevations in winter months demonstrated a similar trend as in KC-U1, and the lowest level was found in summer months (figure 11, 12). The OC/EC ratio of this source is 13.5, slightly higher than that in KC-U1. Although the regression coefficient between KC-U1 and KC-P1 is 0.98 (Figure 14), their contributions to the total $PM_{2.5}$ varies. The monthly $PM_{2.5}$ of KC-P1 was 2.05 µg/m^3, which was 46% less than them at KC-U1. The source profile indicated less OC contribution in this source compares to KC-U1, consider the slightly lower OC/EC ratio, it is reasonable to assume that KC-P1 included less secondary aerosols than KC-U1.

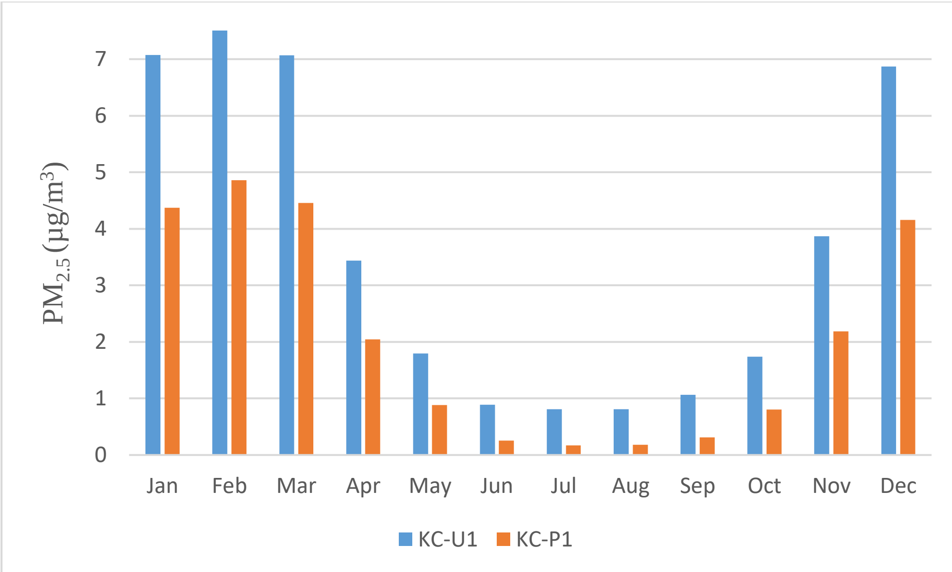

Figure 12 Monthly nitrate/agricultural $PM_{2.5}$ (in μg/m^3) comparison at the Kansas City site.

KC-P2: Sulfate/Industrial

Sulfate/industrial source is the leading contributor to ambient $PM_{2.5}$, identified by high loadings of sulfate. About 2.0 μg/m^3 sulfate contributed to this source, occupied 46% mass fraction in sulfate/industrial source. OC is the second major species in this source, 0.72 μg/m^3 occupied 20% mass fraction of sulfate/industrial source. And the OC/EC ratio is 10.6 in KC-P2, which is lower than that in KC-U2. Monthly $PM_{2.5}$ showed a stable increasing trend from January and reaches the highest level in September. A rapid cutback was seen in October, with the lowest level in October as well. Compare the monthly $PM_{2.5}$ with KC-U2, sulfate/industrial $PM_{2.5}$ from PMF model is slightly lower than that in the Unmix model from April to November. As mentioned before, the formation of secondary ammonium sulfate is enhanced during warm months, it is believed that the KC-U2 accounted for more secondary aerosols than the KC-P2 (figure 13). The similar analogies were also seen in KC-U1 and KC-P1. Times series data shows a decreasing trend after 2005, comparable with both model results from the Flint Hills site, and KC-U2. Overall, the KC-U2 and KC-P2 carried a 0.93 regression coefficient in source contributions (figure 14).

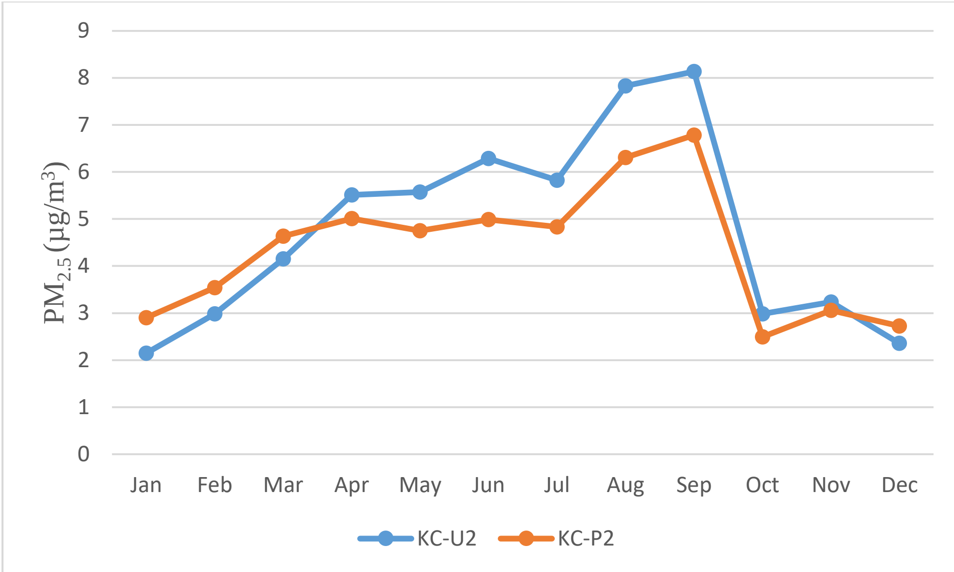

Figure 13 Monthly sulfate/industrial $PM_{2.5}$ (in µg/m^3) comparison at the Kansas City site

KC-P3: Crustal/Soil

Crustal source contributed 9% ambient $PM_{2.5}$ at Kansas City site, almost three times than it in Unmix model result. This source gathered more than four-fifths Si (0.1 µg/m^3) and Al (0.02 µg/m^3), and about a quarter Fe (0.02 µg/m^3). Time series and monthly $PM_{2.5}$ level showed a similar trend with KC-U3. A rapid increase was found in July, where the monthly contribution was over two times higher than the contribution of any other month. The combination of OC and EC occupied 35% mass fraction of this source. Since the suspended crustal dust was considered a potential source of secondary organic aerosol (Jeong et al., 2016), it is possible that KC-P3 accounted suspended dust as crustal/soil source, while KC-U3 include the dust into other SOA featured categories.

KC-P4: Smoke

Smoke tracer K_{non} was again used in identifying the smoke source, with 89% (0.09 µg/m^3) K_{non} contribution. OC was the leading contributor that occupied 38% (0.44 µg/m^3) mass fraction in the smoke source. The time series plot and a monthly contribution of this source were almost identical with KC-U4, supported by the regression coefficient of R^2=0.99 (figure 14). Peak values all appeared to be around the 4th of July. The averaged $PM_{2.5}$ contribution in July was 3.4 μg/m^3 in KC-P4 and 3.8μg/m^3 in KC-U4, which were both more than two times higher than any other months. The OC/EC ratio was exceedingly high, indicating the existence of large amount SOA. Unlike the Flint Hills site, the prescribed burning did not bring an intensive rising in Kansas City smoke source.

KC-P5: Traffic/SOA

Traffic/SOA source contributed 25% ambient $PM_{2.5}$ in the PMF model. The carbonaceous species (OC and EC) has taken 75% mass fraction in this source, in which OC is more than seven times than EC. This was then identified as SOA originated source due to the high OC/EC ratio. The enriched Zn (51%), Mn (61%), Fe (35%), and Ca (6%) were elements implying the effect from diesel profile. Due to the EPA requirement of phasing-out of lead in all grades of gasoline, lead (Pb) was absent in this source. No regular pattern was recorded in time series plot. The monthly contributions of KC-U5 and KC-P5 were not quite harmonized as other sources. The greatest separation was observed in July, which was also the high loading month of crustal/soil source. Recall KC-P3, the $PM_{2.5}$ level in July had a 1.89 μg/m^3 surplus than KC-U3, while the averaged surplus (monthly average of KC-P3 subtract KC-U3) was 0.81 μg/m^3. Due to the above evidence, it is possible the two models handle SOA in July differently between crustal/soil and traffic/SOA sources.

KC-P6: HDDV

The heavy-duty diesel vehicle source contributed 9% mass percentage of $PM_{2.5}$ at the Kansas City site and was determined based on multiple clues. The leading species revealed the combustion properties were carbonaceous species, especially OC; 0.87 μg/m^3 OC weighted 70%

of the mass fraction of this source. High loadings of Fe and Mn could be from diesel additions. No obvious pattern was observed in either time series plot or monthly contributions.

KC-P7: Cu dominated

Cupper dominated source was identified by Cu, 89% Cu was included in this source. The highest record of KC-P7 was found in July, same as in KC-U7. The absolute $PM_{2.5}$ level in this source was slightly lower than the KC-U7, but the overall tendency agrees well each other (R^2=0.99).

Comparison of Unmix and PMF modeling results at the Kansas City site

The Unmix and PMF resolved a same number of factors at the Kansas City site, source contribution and composition are in accordance with nitrate/agricultural, sulfate/industrial, smoke, and Cu dominated categories. However, the two models tend to treat SOA in divergent ways. Secondary aerosols from the traffic originated source are often formed from the oxidation of SO_x, NO_x, and the neutralization of NH_3 (Seinfeld and Pandis, 2016), and possibly be broken down and concluded in various categories. The regression coefficient of crustal/soil between two model results was 0.6978, it is likely due to different SOA processing between models. For instance, source composition of KC-U5 (traffic/SOA) and KC-P5 were in low agreement (P=0.18), the combination of soil, traffic/SOA, and Cu sources from Unmix (KC-U3, U5, and U7) and PMF (KC-P3, P5, P7) carried a high correlation coefficient (P=0.46). The comparison analysis between model-derived $PM_{2.5}$ sources would be a progressive approach in quantifying SOA. Furthermore, the Unmix and PMF models resolved a highly consistent solution in categories with unique tracer element, e.g. K_{non} in the smoke category.

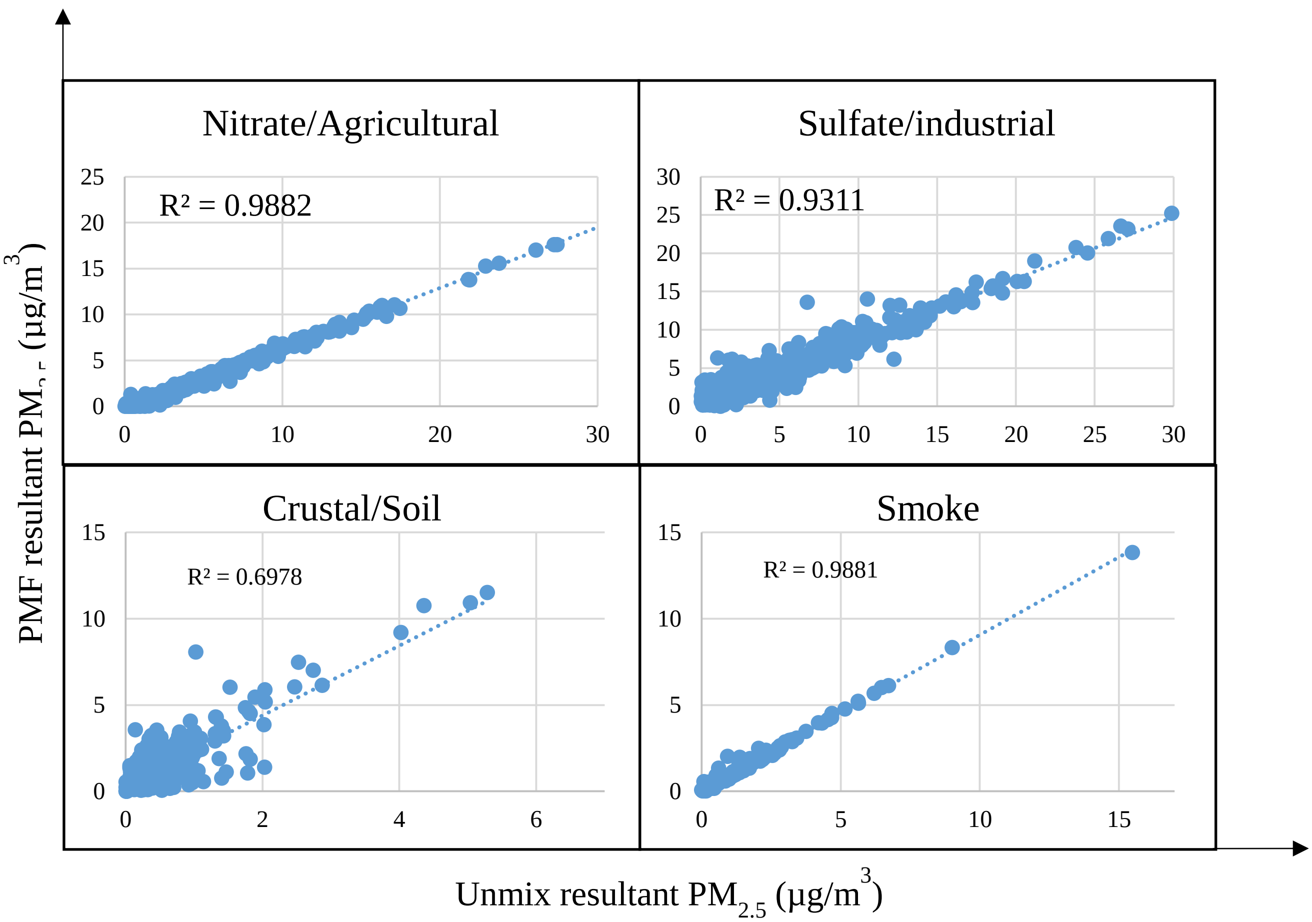

Figure 14 Comparison between Unmix and PMF results at the Kansas City site

1.4.3 Site comparison

Both receptor models revealed interpretable results in the two sites, with the annual averaged ambient $PM_{2.5}$ at the Kansas City site higher than the one at the Flint Hills site. The source apportionment demonstrated more complicated source categories at the Kansas City site than that at the Flint Hills site. The common sources shared by the two sites were nitrate/agricultural, sulfate/industrial, crustal/soil, smoke and traffic/SOA.

As leading species, OC level at the Kansas City site was more than three times higher than that at the Flint Hills site, which suggested more SOA precursors in the urban area. In nitrate/agricultural and sulfate/industrial categories, the OC/EC ratios were much higher than at the Kansas City site, and the mass fraction of carbonaceous species (EC and OC) at the Kansas City site were about two times higher than in Flint Hills rural site. The crustal/soil and traffic/SOA source categories also had a higher OC taking up at the Kansas City site, indicating more SOA formation. The smoke source category FH-P4 contributed about 20% of the total $PM_{2.5}$, while KC-P4 only accounted for 9% ambient $PM_{2.5}$. Peaks of FH-U4 and FH-P4 were in the month of April when the prescribed burning was taking place, while peaks of KC-U4 and KC-P4 were observed in the month of July, potentially due to campfires or the fireworks around the 4th of July celebration. The previous study also addressed the enhanced biomass burning contribution in rural than in urban locations (Kundu and Stone, 2014). Moreover, the smoke category at the Flint Hills site contained more EC, which are likely emitted directly from combustion (FH-P4: EC/total=7%; KC-P4: EC/total=1%). In contrast, the smoke category at the Kansas City sites contained more OC and sulfate, indicating more secondary aerosol formations.

Radar charts were used to illustrate the average source contributions of selected source categories under various wind directions at both sites based on the PMF modeling results (figure 15). The nitrate/agricultural source category had a notable higher contribution under the north wind. Higher contributions in the sulfate/industrial (P2) and crustal/soil (P3) source categories were observed under the south wind at both sites; this could due to coal-fired power plants, such as the La Cygne Station (Linn County) and the Empire District Electric Co. (Cherokee County), located in the south of the Kansas City sampling sites. Higher contributions were observed at the Kansas City site in the nitrate/agricultural, sulfate/industrial, crustal/soil, and traffic/SOA categories (P1, P2, P3, and P5) under every wind directions, except the smoke source category (P4). FH-P4 had higher contributions under southeast and south wind directions, while KC-P4 had higher contributions under southwest and west wind direction.

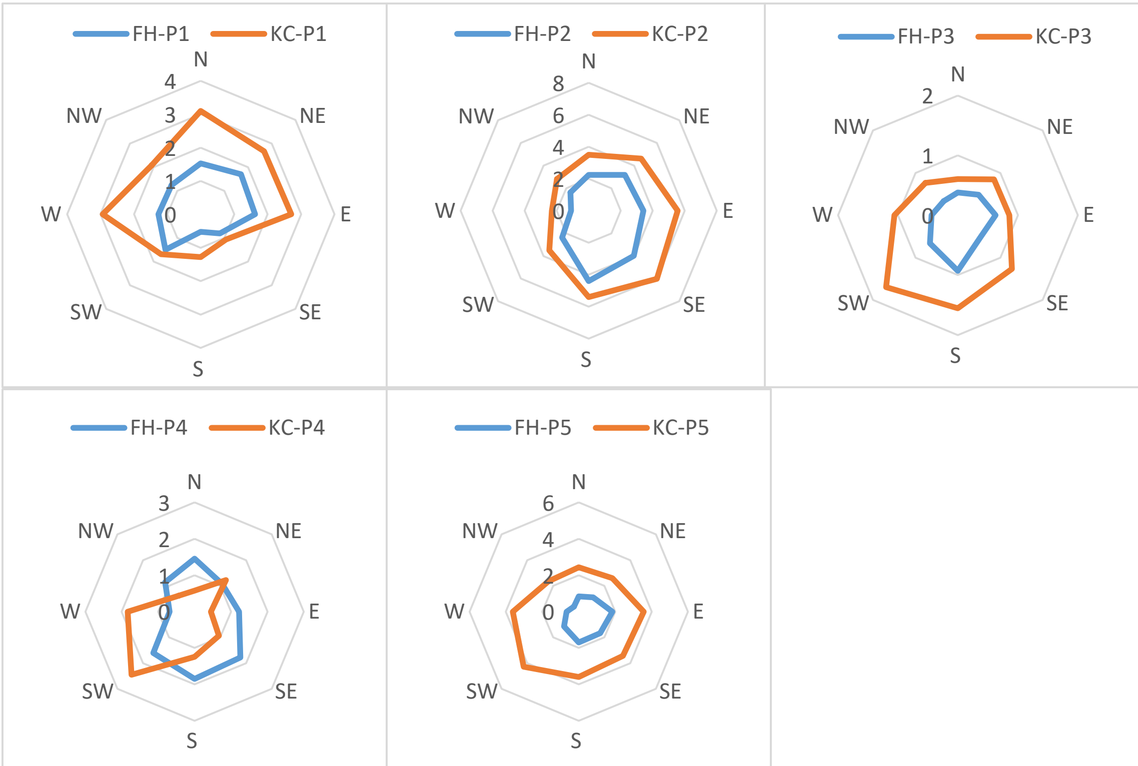

Figure 15 Average contributions of selected categories (in µg/m^3) by wind directions.

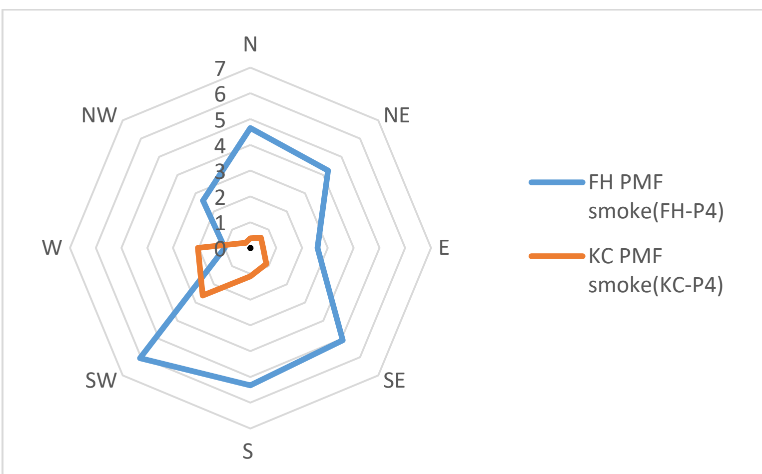

Figure 16 Smoke originated $PM_{2.5}$ (in µg/m^3) distributed by wind direction during the burning seasons.

Figure 16 is a radar chart illustrating contributions of the smoke source categories under various wind directions at both sites using multi-year data during the burning seasons (from March 15 to May 14). During this period, a relatively high correlation (Pearson coefficient = 0.6) was found between FH-P4 and KC-P4 when Kansas City was under the influence of west and southwest wind (wind direction: 202.5°-292.5°). The KC-P4 showed a prominent high contribution under the southwest wind, suggesting that part of the smoke originated $PM_{2.5}$ in the urban site could have come from the upwind burning activities.

1.4.4 $PM_{2.5}$ source impacts on visibility degradation in rural and urban Kansas

Temporal variation of visibility

Annual visibility variations from 2001 to 2016 are compared with those in different seasons, as shown in Figure 17. Seasonal visibility variations were also demonstrated using winter morning and summer afternoon frames. A winter morning was defined as 0600 to 0900 CST in December of the previous year, January, and February. Summer afternoon was denoted as 1500 to 1800 CST in June, July, and August.

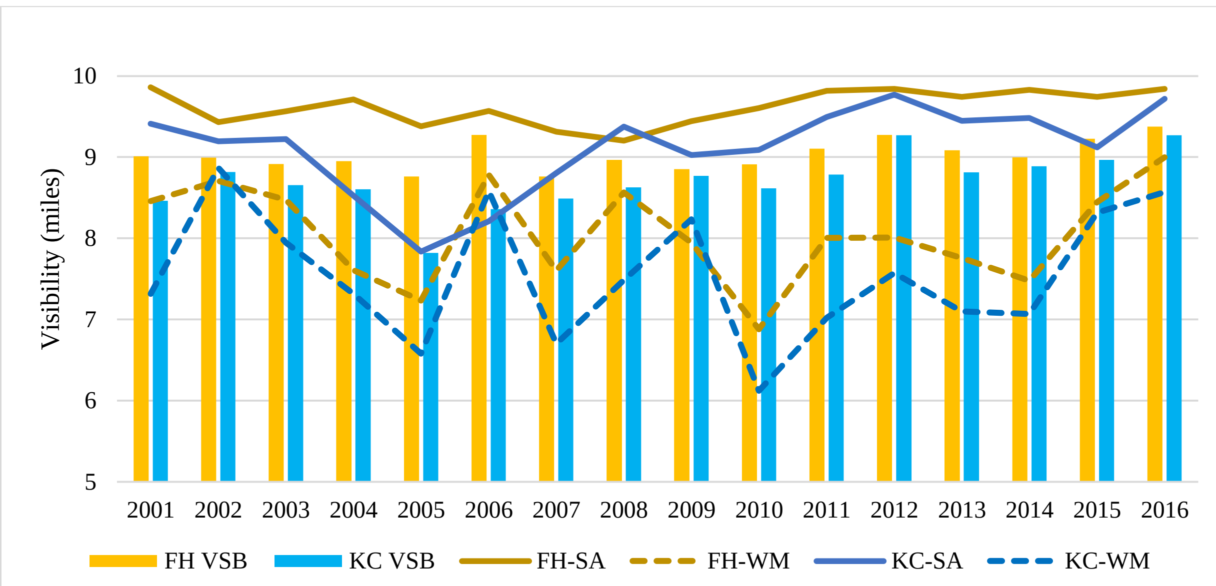

*FH VSB: Flint Hills annual averaged visibility. KC VSB: Kansas City annual averaged visibility. FH-SA: Flint Hills summer afternoon visibility. FH-WM: Flint Hills winter morning visibility. KC-SA: Kansas City summer afternoon visibility. KC-WM: Kansas City winter morning visibility.

Figure 17 Annual and diurnal visibility variation in Flint Hills and Kansas City

Visibility in Flint Hills and Kansas City was compared in the histogram (figure 17), with a higher averaged value at the rural site. The multi-year visibility average is 9.03 miles at the Flint

Hills site compared to 8.7 miles at the Kansas City site. In both locations, 2005 carries the lowest annual average visibility, while the best annual visibility was in 2016.

Overall, an increasing trend in visibility was found throughout these years, with the rate of increase higher in Kansas City than in Flint Hills site. An obvious degradation occurred in 2005 (Figure 17), where the annual visibility was down to 8.76 miles, and 7.82 miles at the Flint Hills and Kansas City sites, respectively. One possible explanation might be the prescribed burning event in 2005. From the satellite imagery analysis, there were 3.5 million acres pasture burned in 2005, while the average annual (2003-2014) burning area is around 2.2 million acres. Differences of the annual extreme values at the Kansas City site (1.45 miles) is more than two times than it at the Flint Hills (0.62 miles), demonstrating a greater disparity and implicating a more complex air pollutants composition.

The summer afternoon visibility from both locations as shown in Figure 17 in solid lines, with the majority of values are higher than the annually averaged visibility. On the other hand, the winter morning visibility is usually lower than the annual average values for most of the year. A special case was observed in 2006, likely due to the low averaged RH in winter of that year. Typically, a higher particle level in winter morning is devoted of low mixing height, high RH (Ghim et al., 2005; United States Bureau of Land Management, 2008), and frontal passages (Davis, 1991), which led to visibility impairment during this time. Photochemical reactions formed secondary aerosols in summer afternoons potentially affected visibility, while the high mixing height improves visibility at the same time. The higher mixing height in summer afternoons is more effective than the secondary particle formation in photochemical reaction, therefore, maintained the visibility higher in summer afternoons than in winter mornings. The summer-afternoon visibility distribution at the Kansas City site spanned a wider range along the y-axis compared to the Flint Hills site. This is likely due to the high density of anthropogenic emissions contribute to a greater visibility variation. Tsai and Cheng (1999) reported visibility differences between weekdays and weekends in an urban area. No similar discrepancy was found in either urban or suburban region from this work.

Effects of meteorological parameters on visibility

The study revealed the visibility is under the influence of local liquid and solid precipitation, especially when the air temperature is low (Gultepe and Isaac, 2006). The current data set indicated a significant difference in both locations with or without precipitation. The visibility range is 0.5 miles shorter on rainy or snowy days in Flint Hills, while in Kansas City, the difference developed to 0.86 miles. Theoretical calculations of the relationship between precipitation and visibility have been performed in several studies (Gultepe and Isaac, 2006; Rasmussen et al., 1999), but the result has shown a large variation. Detailed weather conditions, such as rain intensity, droplet sizes, and precipitation duration could help quantify the relationship with visibility.

Relative humidity is one of the key factors of visibility variations, with a large range from 14% to 100% in the datasets. Segmented RH was used to coordinate with the visibility data. A cutoff RH value was observed in the dataset. When RH is lower than 50%, no significant influence on visibility was observed, while when RH is higher than 50%, a significant negative association was found between RH and visibility. This is because the $PM_{2.5}$ particulates absorb moisture and causing light scattering (Lee and Cheng, 1996; Malm and Day, 2001). It is understood that a high RH weather condition could keep more suspended particles, and benefit light scattering. Consider non-precipitation days with RH greater than 50%, the correlation coefficient between RH and visibility is -0.3 in Flint Hills and -0.4 in Kansas City. Visibility at both locations reveals an obvious decline in 2005. The comparatively high RH in this year could be one of the reasons. Note that RH is not the only contributor to visibility degradation, other causes such as population density, traffic emissions are also a notable source of pollutants (Tsai and Cheng, 1999). To look at the entirety RH through multiple years, a coincided relationship between all range RH and visibility are appeared in the Flint Hills data, with correlation coefficients of -0.6. The correlation coefficient between RH and visibility in Kansas City during the same period was only -0.2, indicating the RH variation in an urban area is not as influential as in suburban.

Although temporal and meteorological parameters have been illustrated powerful effect of visibility, the vital influence from particulate matter cannot be left out.

Tobit model and effects of $PM_{2.5}$ sources

For both locations, the Unmix modeling results have less negative values than the PMF modeling results. Thus, the Unmix resultant sources were used to coupling with visibility and other climatological parameters. Hourly visibility data were averaged in each day to correlate with the 24-hour speciated $PM_{2.5}$ level.

Scatter plots were employed first to investigate the $PM_{2.5}$ impacts. Figure 18 displayed the correlation between ambient $PM_{2.5}$ and daily averaged visibility on both sites. Low visibility (visibility < 3 miles) values are often corresponding with high RH (>70%) winter days, which could be explained by the seasonal and RH effects. Meanwhile, days with $PM_{2.5}$ concentration more than 40µg/m^3 were always coupled with relatively low visibility values. This is implying the importance of PM effects on visibility degradation.

Visibility in figure 18 was not equally distributed along the y-axis, but more centered by 10 miles mark. This is due to the measuring method, which records visibility more than 10 miles as 10 miles. As such, the input data was right censored. In order to analyze the impact factors of visibility, the entire data set needs to break down into two parts, values recorded as true and values over the upper limit 10. Tobit model was introduced in dealing with the piecewise function of visibility.

$$y_i = \begin{cases} y_i & if\ y_i < y_L \\ y_L & if\ y_i \geq y_L \end{cases} \quad \textbf{(3)}$$

As in Equation 3, the Tobit model was designed to estimate the linear relationships between variable when there is a left or right censoring in the dependent variable, which is visibility in this case. The historical weather data and receptor model derived $PM_{2.5}$ sources were used in the Tobit model analysis. Table 9 listed significant visibility impact factors from two locations, and their parameter estimations.

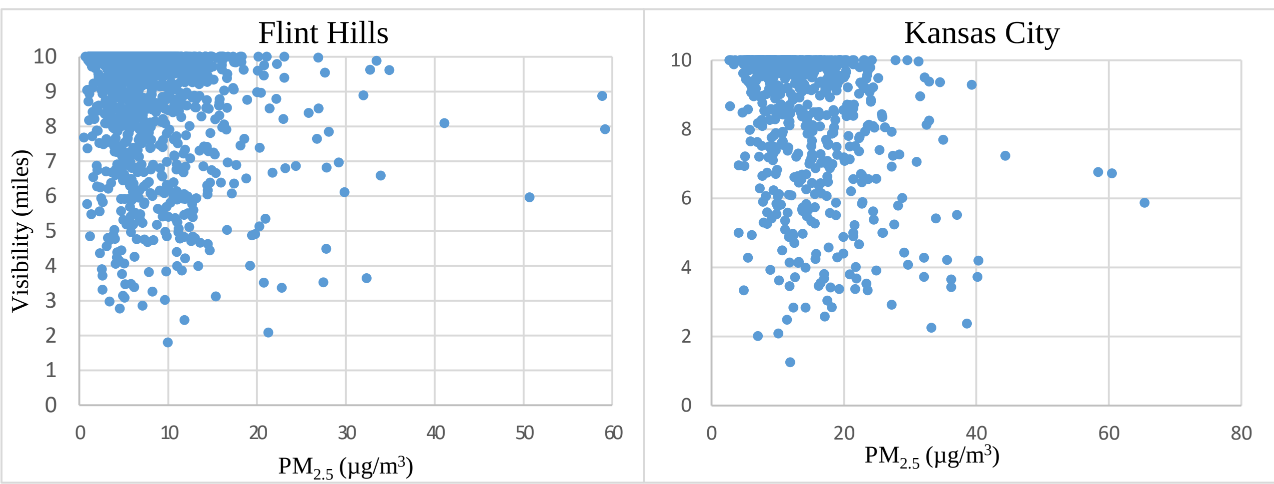

Figure 18 Scatter plots between ambient $PM_{2.5}$ and visibility from Flint Hills rural and Kansas City urban sites.

Both locations demonstrated nitrate/agricultural originated $PM_{2.5}$ as the greatest impact factor that negatively correlated with visibility range. When agricultural $PM_{2.5}$ reached 10 µg/m^3, the negative relation enhanced with correlation coefficient equals to -0.4 in Flint Hills and -0.43 in Kansas City. The agriculturally generated fine particles are mainly secondary aerosol. The precursor particles emitted from this source have a far-reaching effect under the influence of photochemical reaction in the troposphere. A regular seasonal pattern of agricultural originated $PM_{2.5}$ was seen in the time series with ceiling values in winter (Dec. to Feb.) and minimum values in summer (Jun. to Aug.). The regional agricultural ammonia emission supported the secondary nitrate formation; meanwhile, the weather condition such as low wind speed, low temperature, and stagnant condition act as drivers of this episodic pollution. In Flint Hills site, industrial, smoke and SOA were $PM_{2.5}$ sources identified as visibility impact factors. The only influentially meteorological parameter was RH. At the Kansas City site, wind speed and maximum air temperature were considered influentially meteorological factors, but less $PM_{2.5}$ sources were included in the table. The different visibility impact factor could be explained by the urban area features. The urban environment is kept warmer because of more paved surfaces and more CO_2 emitted from anthropogenic sources, which is in favor of SOA formation. The stagnant conditions in an urban area are also persistent during the day because of larger-scale wind patterns (Chen et al., 2011). The parameter estimation in Table 9 was provided by the Tobit model analysis, indicating the magnitude of each factor's influence (in the range of 0-1) to visibility impairment.

Table 9 Visibility impact factor and parameter estimations in the Tobit model.

Flint Hills	Parameter estimation	Kansas City	Parameter estimation
Nitrate/ Agricultural	-0.29	Nitrate/ Agricultural	-0.31
Sulfate/ Industrial	-0.24	Wind speed	0.21
Smoke	-0.18	Sulfate/ Industrial	-0.15
RH	-0.06	Max air temp.	-0.03
SOA	-0.05	RH	-0.01

1.5 Conclusions, limitation, and future work

The application of both Unmix and PMF models at the Kansas City site resulted in 7-source solution (nitrate/agricultural, sulfate/industrial, crustal/soil, smoke, traffic/secondary organic aerosol (SOA), diesel/heavy-duty diesel vehicles (HDDV), and Cu dominated source) that contribute to ambient $PM_{2.5}$.

Comparative analysis at the Flint Hills site provided more hints on the relative contribution and characterization of primary and secondary smoke aerosols. Smoke sources in the Flint Hills performed various features in Unmix and PMF model. The primary and secondary aerosols from the smoke source were identified as separate sources in Unmix result, and SOA from other origins was also mixed in the burning-related SOA category. However, the PMF model was more preponderant in identifying the smoke-related category as an entire body. Both primary and SOA from burning were accounted into one source, while SOA from other cause was indexed into separate categories. In April, the burning originated secondary aerosols is estimated 2.3 to 2.7 times of the primary aerosols. By computing source contributions in FH-U4 and FH-P4, smoke from prescribed burning accounted for 40% of total ambient $PM_{2.5}$ in the months of April.

In comparison with the Flint Hills site, the Kansas City site carried a more complex source component. As the SOA precursor, the OC in urban site almost doubled its contribution. More paved road and gypsum materials in the urban environment led to a different source composition in crustal/soil, and traffic/SOA sources. The PMF results at the Kansas City site tend to classify more SOA from nitrate/agricultural and sulfate/industrial sources into traffic/SOA source. Although smoke sources were carried in both site, the peak value and major donor were dissimilar. The smoke source at the Kansas City site elevated in July, and can be explained by fireworks on the Independent Day celebration, and possible campfires. The smoke source at the Kansas City site also carries an exceedingly high OC/EC ratio, which is more than five times higher than it in Flint Hills site. Traffic/SOA $PM_{2.5}$ source (KC-U5, KC-P5) found more trace of mobile origins, some traffic originated SOA were even observed in crustal/soil source (KC-P3).

The two receptor models provided a more comprehensive information on source profiles and source contributions. Because the Unmix model separate source based on time sequence, it is in favor of identifying the later formed SOA from burning event. Moreover, during the burning season, the smoke source from both sites carried a relatively high correlation when KC is under west and southwest wind, suggesting that part of the smoke originated $PM_{2.5}$ at the urban site could be from the upwind burning activities. Multiple power plants in southern Kansas might have effects in the $PM_{2.5}$ industrial source to both sites. Source profiles derived in this work may provide a reference in applying the emission-based model in the future. Tobit modeling was used in identifying visibility impact sources. Both climatological parameters and particle sources were employed in the Tobit model analysis, with nitrate/agricultural source being the leading degradation contributor in both sites.

This study provided a more reliable source apportionment study by using multiple receptor models. However, the receptor model is not the best practice in partitioning low strength sources, more detailed sources could be derived from sulfate/industrial, and traffic/SOA categories. In addition, the hourly visibility data were found associated with ozone concentration; data in this study could be used to analysis weekend effect.

There are opportunities for future work emerging from this research: a more accurate prescribed burning details could be monitored in daily satellite images. These field details will help in explaining and validating the apportioned smoke source contributions. SOA management strategies are under pressing need in order to reduce air quality impact from prescribed burning. And the complete meteorological predictor can be included, such as mixing height to show the atmosphere stability.

Chapter 2 - A review of life cycle assessment on the carbon footprint of beef production in the U.S.

2.1 Introduction

Greenhouse gas (GHG) emissions from agriculture, forestry, and fisheries have roughly doubled over the past fifty years based on estimations from the Food and Agriculture Organization (FAO, 2014). The agricultural GHG emissions in the US are about 563 million metric tons (MMT) of CO_2 equivalent in 2016, and accounting for 8.6% of the total GHG emissions (EPA, 2018). Agriculture is responsible for a significant portion of anthropogenic GHG emissions, there is also an opportunity for some mitigation to be achieved by conducting better agricultural management. The agricultural GHGs include CO_2, CH_4, and N_2O, and their leading sources are N_2O released from soil related to N fertilizer usage (38%), CH_4 from livestock enteric fermentation, N_2O from manure management (38%) (Scheehle et al., 2006). In particular animal production systems in the US, beef cattle are by far the largest CH_4 emitter. The beef cattle emitted 121 MMT CO_2 equivalent in 2016, accounting for more than 71% of the total anthropogenic CH_4 emissions in that year (EPA, 2018).

The complexity of livestock operation systems and differences of ecological systems, presence challenge in keeping accurate and precise emission records of each GHG component. To evaluate GHG emissions from livestock production, it is essential to use a whole system modeling approach (Stewart et al., 2009). Life cycle assessment (LCA) in livestock production system is widely accepted in assessing the environmental impacts throughout the entire production's life (cradle-to-grave) (ISO, 1997). By using the LCA procedure in animal production systems, researchers could identify the system components and key leverage points for reducing environmental impacts in the production system, also quantify life cycle emissions for comparison between different aspects (Dudley et al., 2014). There are two types of LCA studies commonly used in a beef production system: attributional LCA (aLCA) and consequential LCA (cLCA). The aLCA describes the average environmental impacts representing a given production system; while the cLCA aimed at quantifying the environmental consequences of a change in demand for a product (Thomassen et al., 2008). Carbon footprint (CF) is an indicator of environmental impacts in LCA studies (Röös et al., 2013) such as GHG emissions, energy consumed and land usage. In this study, the CF estimates both direct and indirect GHG emissions in the production process (Desjardins et al., 2012). Direct comparison among studies' results is almost impossible since LCA studies employed different system boundaries and the analytical context.

Objectives

The objectives of this study were to evaluate carbon footprint range in beef production from different LCA studies, identify the leading CF contributor and dominant source of uncertainty, and summarize the LCA inventory defined in cattle production systems.

2.2 Database selection and literature search

The number of journal articles addressing LCA of beef has increased considerably over the last twenty years. The initial literature search was conducted among three commonly endorsed database: Scopus, Web of Science, and CABI. The literature search with the keywords "life cycle assessment", "carbon footprint" and "beef" in title, abstract and keywords were applied in this database. As shown in table 10, the Web of Science database carries the most number of articles, which is more than three times than the CABI database. In order to eliminate counting the duplicated articles, the following study will focus on articles found in the Web of Science database.

Table 10 Number of articles published each year in the databases, citing "Life Cycle Assessment", "carbon footprint", and "beef" in title, keywords or abstract.

Publication year	*Web of Science*	*Scopus*	*CABI*
2010	1	1	1
2011	4	2	3
2012	8	6	3
2013	4	3	1
2014	5	2	1
2015	6	7	3
2016	9	4	1
2017	13	9	3
2018	7	4	0
Total	57	38	16

The leading journal representing beef LCA studies was the Journal of Cleaner Production, with 15 publications (26%). The European Union had the highest number of publications in the beef LCA field, but the U.S. is accounted for 13 (23%) publications acted as the leading country. A literature search using earlier terms of LCA such as environment profile analysis, environmental profiling and cradle-to-grave assessment (Roy et al., 2009) was also applied, the searching result was combined in the following analysis.

To further identify suitable studies, an abstract filtering was carried through within the publications found in Web of Science. The literature inclusion criteria were: the study must have simulated or measured CF data which can be expressed in the LCA function unit, and the study must be a peer-reviewed journal article in English. The US LCA studies covered farms from 30 states, which are highlighted in figure 19. A data extraction sheet was developed for consistency.

The LCA study inventory was recorded in categories like geographic region, cattle raising system, system boundaries, CF method, CF range, function unit, dressing percentage, etc.

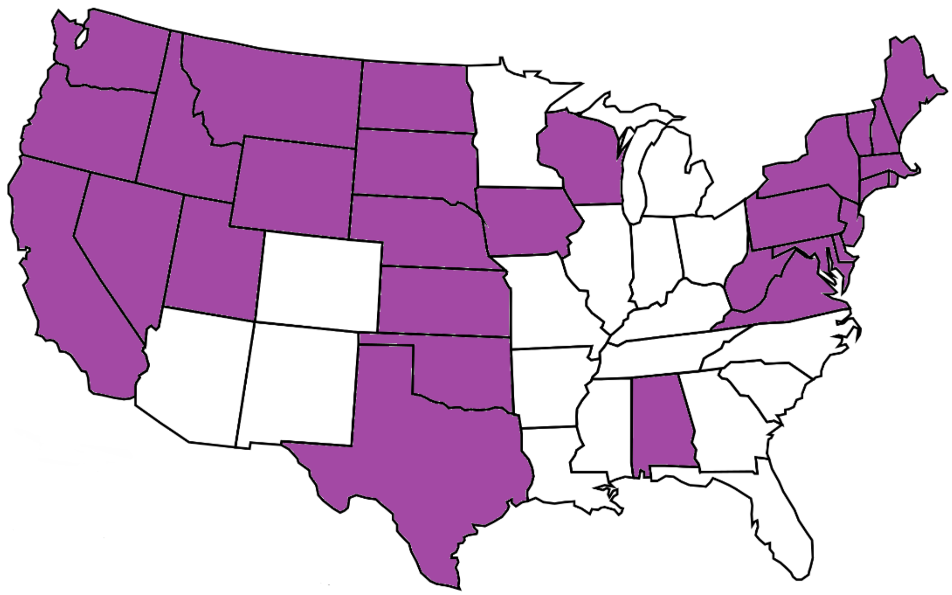

Figure 19 Geographic locations of LCA studies in the U.S.

2.3 Review of LCA inventory

2.3.1 LCA goal and scope

The goal and scope, namely the frame and foundation, describe the specific interest and the depth of an LCA study. In some cases, they are established in LCA model assumptions. The LCA goal defines whether it is an attributional LCA or a consequential LCA. The study objectives are the most important component of an LCA because the entire project was carried out according to its statement. The study objective of an attributional LCA is to quantify environmental impacts from the production system; while the objective of a consequential LCA is to evaluate the expected consequences of a change in the production system (ISO, 2006). Only attributional LCA studies were considered in this project. The scope defines details of the study to sufficiently meet the stated goal, such as system boundary, function unit, and allocation method.

The selected LCA publications in present work address the carbon footprint of beef production systems all over the world aiming at systematic GHG emission, CF uncertainties, allocation methods etc. More than half of the literature included in this review were aiming at comparing environmental impacts between various beef production system. This various features in raising system, feeding component, locations, and cattle types. In addition, LCA applications are also focusing on other environmental impacts, such as energy consumption, acidification, eutrophication potentials, and land occupation (Bragaglio et al., 2018; Nguyen et al., 2010; Röös et al., 2013; Subak, 1999).

2.3.2 System boundaries and beef raising system

The system boundary defines which elements in the beef production system are included in the LCA. Ideally, every stage of the production system should be included, from raising a beef calf to food waste estimation. However, the limited resources should be devoted to significantly influential aspects. System boundary in the research is usually a reflection of goal and scope and is decisive for the results. To determine the significance of a process in the system prior to LCA analysis is difficult, once a process is well studied, there is no point to leaving this process out. In most cases, the initially defined system boundary would need to be refined subsequently (ISO, 2006). Most of the included studies followed a cradle to farm gate LCA. Few of them include activities beyond farm-gate. Roop et al. (2014) used a cradle to processing gate system boundary and estimated the contribution of the post-farm process to overall CF was less than 10%. The inclusive US studies often neglect GHG emission related to capital goods and machinery, only a few studies from European accounted for emissions related to capital goods, buildings, and machinery (Williams et al., 2006). A typical beef production system in LCA has primary inputs in the beef production systems such as feed, water, energy usage (electricity and fuel), and secondary inputs such as crop growing essentials (fertilizer, pesticides, irrigation water, and crop energy consume),and transportations (feed and animal) (Capper, 2011).

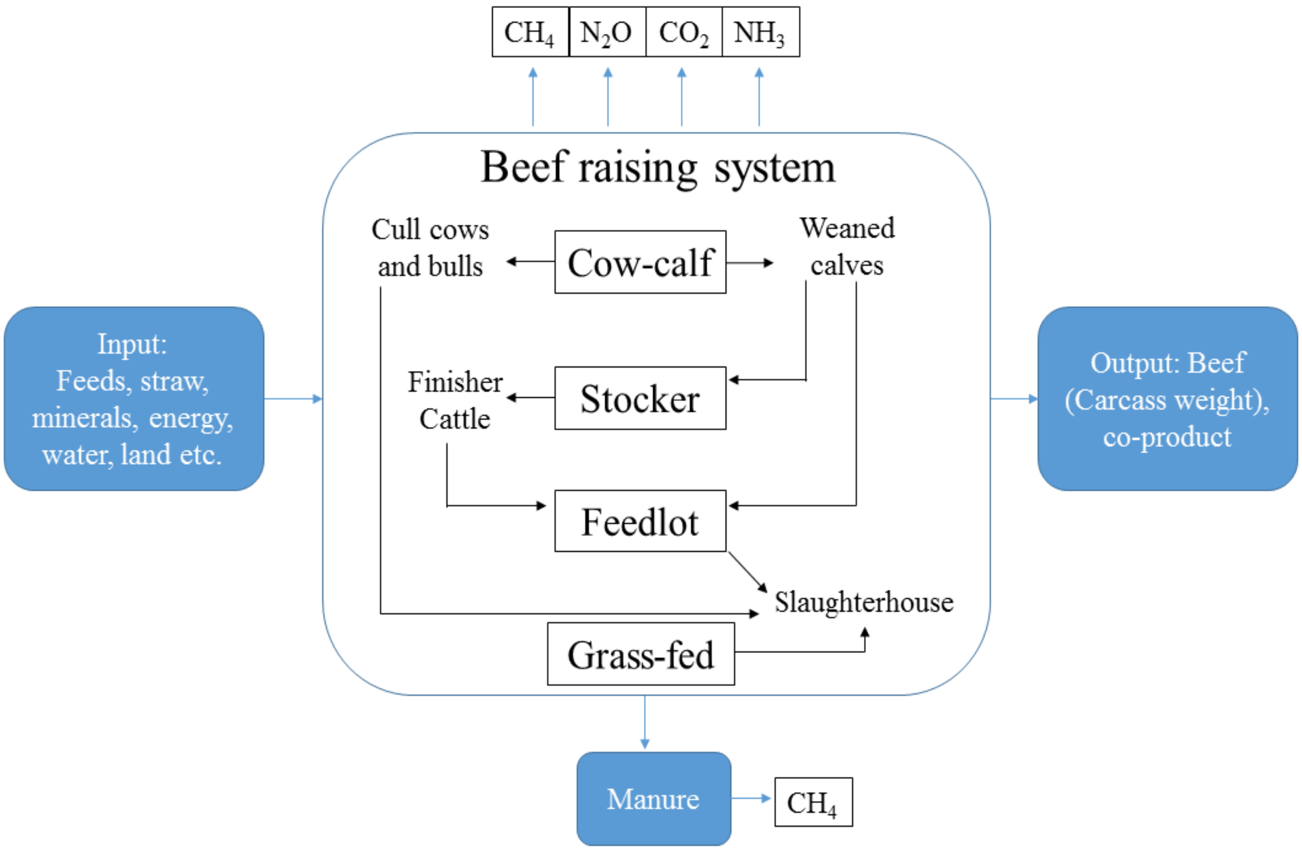

Figure 20 Beef raising system and system boundaries from inclusive LCA studies.

In 2016, the US was the greatest beef producer in the world with 92 million head of cattle and calves (USDA-NASS Census of Agriculture). Figure 20 displayed the concept of beef raising system and system boundaries seen in the inclusive LCA studies. Beef cattle are present in every state in the US, but the numbers, farm scale, and raising the system highly depend on regions. Two-phase and three-phase (namely conventional) beef production systems were the preponderance in the US beef operations. The conventional beef production systems usually consisted of cow-calf phase, backgrounding/stocking phase, and feedlot finishing phase (Capper, 2011); while in a two-phase system, the weaned calf from the cow-calf facility was sent to feedlot finishing directly. Grass-fed cattle were referred to beef production based on pasture or organic systems, which comprise only 3% of today's beef production (Johnson, 2010). Although farms may apply the same production phases in raising cattle, the growing period and feed composition of each phase could vary, and then led to dissimilar CF result.

2.3.3 Method of allocation

In the beef production systems, there are both products and co-products, such as beef, veal, and milk on a dairy farm. The process of appropriately assigning environmental impacts, the CF in this case, to each product is called allocation. By extending the system boundaries, allocation could be avoided, but to study a specific product, beef, for instance, a constant and reliable allocation method should be determined.

The allocation method could be biophysical based or economic value. A biophysical based allocation uses energy, or nutrition content associated with products to assign the environmental impact; while an economic value based allocation is usually weighted by mass (Environmental Working Group, 2011). The mass-weighted economic value has proved to be a reliable allocation method. Stackhouse at al. (2012) used this procedure in determining CF of calves when leaving the dairy farm. Other inclusive studies that applied the mass-based allocation method are Roop and Rotz (2014; 2010). Pelletier et al. (2010) chose the biophysical allocation method using gross chemical energy content in appointing environmental footprint into different beef operations. A similar allocation method was also used by Rotz and Lupo's (2013; 2015).

In summary, the greater part of the CF study was designed on comparing different beef production systems. There are only a limited number of LCAs that are focused on a specific whole farm-level CF with itemized breakdowns. Because of the abounding specifics mentioned in the LCA inventory, CF value from original study results cannot be compared without considering these fine points. Comparison between production systems can be helpful in identifying a better agricultural practice, in finding a more efficient feeding plan, or in ensuring the cattle genetic selection. However, in order to increase the standardization of LCA inventory specifics and make the CF results directly comparable, a great number of whole-farm analysis with itemized emission breakdowns of a specific region are required.

2.3.4 Greenhouse gas emission assessment in LCA studies

The method for calculating carbon footprint is sophisticated because the GHG emitted and embodied from each stage in the LCA need to be taken into consideration. A standard calculation method of CF is still evolving (Pandey et al., 2011), the current LCA studies estimate the GHG emissions by using the Intergovernmental Panel on Climate Change GHG emission algorithms (Desjardins et al., 2012; Intergovernmental Panel On Climate Change, 2007).

The gaseous emissions included in LCA carbon footprint studies were CO_2, CH_4, and N_2O. CO_2 worked as input in plant photosynthesis, while excreted as a product of animals metabolism. CO_2 emitted directly from cattle can be considered as emission neutrality. GHG emission neutrality indicates the net zero GHG emission from all sectors. For instance, the carbon sequestration into soil has the potential to offset agricultural emissions (Crosson et al., 2011). Enteric fermentation in cattle rumen is the major source of CH_4 emission in beef production. Manure management is another source of agricultural CH_4 emission, especially in liquid manure storage systems under high temperature (Crosson et al., 2011; Mogensen et al., 2015). Although it is not directly associated with cattle, the CH_4 emissions can be considerably high, especially when excreta are stored under anaerobic conditions (Flachowsky et al., 2018; Montes et al., 2013). There is no direct N_2O emission from animals, but N_2O could be associated with manure storage and the following land application (Flachowsky et al., 2018). The N_2O emissions were often seen in other environmental impacts, such as acidification and eutrophication.

Greenhouse gases were expressed in the CO_2 equivalent in the LCA studies when addressing global warming potential. And the equivalent heating potential of CH_4 and N_2O oxide were slightly different in IPCC editions. Table 11 lists these changes and studies based on different global warming potential weighting factors. The variations in CF result due to different GWP factors are not expected to be significant; Nguyen suggested a minor change (3.7%-5.5%) in the CF result due to this reason (2010).

Table 11 IPCC editions of greenhouse gases conversion to CO_2 equivalent

IPCC standard	Methane (CO_2 eq.)	Nitrous Oxide (CO_2 eq.)	References
1996	21	310	(Casey and Holden, 2006)
2001	23	296	(Beauchemin et al., 2011; de Vries and de Boer, 2010; Nguyen et al., 2010)
2007	25	298	(Bragaglio et al., 2018; Cerri et al., 2016; Heller and Keoleian, 2011; Nguyen et al., 2012)
2013	28	265	(Andreini and Place, 2014)

Field-level GHG emissions were often estimated by using equations and emission factors. Carbon footprint estimation has also been commercialized in all the areas of LCA. LCA software has been used to make the CF estimation more practical and precise. Studies included employed several LCA tools, such as SimaPRo, Gabi, and OpenLCA. The most commonly used software is SimaPro. (Desjardins et al., 2012; Dick et al., 2015; Heller and Keoleian, 2011; Lupo et al., 2013; Ogino et al., 2007; Pelletier et al., 2010; Ridoutt et al., 2011; Roop et al., 2013) The literature has shown the advantage in the graphical representation of SimaPro, compare to the graphical output of Gabi (Rice et al., 1997). Consider SimaPro is not flowed diagram based, the details of system boundary in the flow diagram may vary. The drawbacks of SimaPro being the price, which explains the recent popularity of an open-source software OpenLCA. In brief, comparisons between LCA studies on beef production should be made with caution, because of differences in system boundaries, allocation procedures, and other methodological nuances.

2.4 Review and analysis of the Carbon footprint

2.4.1 Function unit and dressing percentage

LCA studies used various function units to evaluate the greenhouse gas emissions. Although the global warming potential of methane and nitrous oxide were converted to CO_2 equivalent, the mass unit of beef production was quite different depends on different studies. For the carbon footprint of beef production, common units used are live weight (LW) and hot carcass weight (HCW, CW). Saleable meat weight was also used occasionally (Cederberg and Stadig, 2003; Peters et al., 2010). The weight of live animal that ends up as the carcass is expressed by LW. Generally, the carcass weight is taken immediately after skinning and evisceration, also known as hot carcass weight. Saleable meat weight highly depends on cutting specifications, such as bone-in or boneless etc. The existence of co-products in the beef production brought discussion in using CF function unit based on live weight, therefore, the function unit used in this work is kg CO_2e kg^{-1} carcass weight.

To prepare different functional units in the CF comparison, dressing percentage and carcass cutting yield were introduced. Dressing percentage describes the relationship between cattle live weight to carcass weight. Dressing percentage can be affected by factors like cattle bred, fatness, whether include hides, head, feet etc. An averaged dressing percentage for cattle is about 50% to

62% (Cornell University, 2012; Peters et al., 2010; Wulf et al., 1999). Carcass cutting yield is the percentage of the carcass that actually ends up as saleable meat, usually about 65-75% (Peters et al., 2010), and about 55%-60% for boneless meat (Wulf et al., 1999). The following Equation 4 demonstrated dressing percentage and carcass cutting yield conversions.

$$\begin{gathered} \textit{Dressing Percentage} = (\textit{carcass weight} \div \textit{live weight}) \times 100 \\ \textit{Carcass Cutting Yield} = (\textit{meat weight} \div \textit{carcass weight}) \times 100 \end{gathered} \tag{4}$$

Dressing percentage and carcass cutting yield could be quite different depending on the region, cattle type, and raising systems. Table 12 lists several published studies that include their dressing percentage in the discussion.

Table 12 Beef dressing percentage used in published carbon footprint studies

Study	Dressing percentage	Country
(Tsutsumi et al., 2018)	56%	Japan
(Desjardins et al., 2012)	60%	Canada
(Rotz et al., 2015)	50% (cull cattle); 62%	U.S.
(Capper, 2011)	62%	U.S.
(Dudley et al., 2014)	63%	U.S.
(Tichenor et al., 2016)	59% (dairy beef); 54% (grass-fed); 50% (cull cattle)	U.S.
(Lupo et al., 2013)	51%	U.S.

For consistency, carbon footprint included in the present study were converted to kg CO_2e kg^{-1} carcass weight using 55% dressing rate, and 70% carcass cutting yield rate.

2.4.3 Carbon Footprint range and breakdowns

Table 13 Overview of carbon footprint range in published beef LCA studies outside U.S.

Study	Country	Raising system	LCA inventory[a]	Carbon Footprint [b]
(Beauchemin et al., 2010)	Canada	Crop-livestock farm finishing (as in 2-phase)	Direct on farm, purchased inputs and indirect nitrous oxide. Excludes capital and machinery.	21.7
(Williams et al., 2006)	UK	[c]Non-organic; 100% suckler; Lowland; Hill& upland; Organic.	Simulated direct emissions, purchased inputs and indirect nitrous oxide emissions. Include buildings and machinery	15.8; 25.3; 15.6; 16.4; 18.2
(Casey and Holden, 2006)	Ireland	Conventional; Organic system.	Direct on farm, purchased inputs emissions. Excludes capital, machinery, and chemicals.	*23.2; 19.9*
(Cederberg and Stadig, 2003)	Swedish	Cow-calf farm finishing all cattle	Direct on-farm, purchased inputs and indirect nitrous oxide emissions. Excludes capital and machinery.	[d]*15.6*
(Nguyen et al., 2010)	[e]EU	Suckler cow-calf system	Direct on-farm, purchased inputs and indirect nitrous oxide emissions	27.3
(Ogino et al., 2007)	Japan	Cow-calf and fattening (as in 2-phase)	Direct on farm, emissions from energy consumption and animal feed	[d]*25.5*
(Ogino et al., 2004)	Japan	Cow-calf to feedlot finishing	Direct on farm, emissions from energy consumption and imported animal feed.	22.6
(Peters et al., 2010)	Australia	Grain-finished; Grass-fed	Simulated direct emissions purchased inputs, and emissions at the processing plant. Excludes capital goods.	9.9; 12.0
(Veysset et al., 2010)	France	Cow-calf; 2-phase 2-phase (beef steers)	(Survey data) Direct emission, purchased inputs and capital. Does not include indirect N_2O.	30.5; 26.6; 27.1

a: partial of this column was derived from (Crosson et al., 2011) b. Function unit in kg CO_2e kg^{-1} carcass weight. Results in italics indicate CF range converted to the carcass-based unit. c: intensive cereal beef finishing d: 70% carcass cutting yield e: EU: European Union

Table 14 Overview of carbon footprint range in published beef LCA studies in the U.S.

Study	Raising system	[a]LCA inventory	Carbon Footprint [b]
(Pelletier et al., 2010)	2-phase; Conventional; Grass-fed	Simulated direct emissions, purchased inputs and indirect nitrous oxide emissions. Excludes capital and machinery.	[c]*26.9;* [c]*29.5;* [c]*34.9*
(Phetteplace et al., 2001)	Conventional	Direct on-farm, purchased inputs and indirect nitrous oxide emissions. Excludes capital and machinery.	[c]28.2
(Dudley et al., 2014)	Conventional *backgrounding CF not include	Direct on-farm, feed production, indirect N_2O, and indirect land use.	[d]14.8
(Stackhouse et al., 2012)	Angus without growth-promoting; Angus with growth-promoting; Angus with growth-promoting and hormones	Model simulated direct emissions and secondary nitrous oxide emissions. Excludes capital goods.	24.2; 22.6; 22.0
(Stackhouse-Lawson et al., 2012)	Conventional; 2-phase	Simulated direct emission, purchased input and indirect N_2O	22.6; 21.2
(Capper, 2012)	Conventional; [e] Natural system; Grass-fed	Simulated direct emission, purchased input, and indirect N_2O.	16.0; 18.8; 26.8
(White and Capper, 2013)	Conventional; Increased ADG [f]; Increased finishing weight.	Simulated direct emissions, purchased inputs and indirect N_2O.	20.1; 18.5; 17.8
(Tichenor et al., 2016)	Grass-fed	Simulated direct emissions, purchased inputs, and land use. Exclude capital goods.	33.7
(Lupo et al., 2013)	Conventional; Early weaning; Fast backgrounding; Grass-fed	Simulated direct emission, purchased inputs and indirect N_2O.	23.0; 24.1; 22.9; 31.6
(Roop et al., 2014)	2 phase (average from 6 farms)	Direct farm GHG emissions, utility and transportation from cradle to farm gate.	[c]*18.9*
(Rotz et al., 2013)	Conventional	Simulated direct emissions and pre-chain sources (gas, electricity, fertilizer, purchased feed, machinery etc.).	[c]*19.85*
(Capper, 2011)	1977 conventional; 2007 conventional	Simulated direct emissions, crop production input, fuel and electricity.	21.45; 17.95
(Rotz et al., 2015)	Integrated 3-phase	Simulated direct emissions, net GHG emission, energy use, and water use.	20.2
(Roop et al., 2013)	Grass-fed on small farms with early slaughtering	Direct farm GHG emissions and purchased inputs.	25.05

a: partial of this column was derived from (Crosson et al., 2011); b. Function unit in kg CO_2e kg^{-1} carcass weight. Results in italics indicate CF range converted to the carcass-based unit; c: 55% dressing percentage; d: backgrounding phase is not included; e: a conventional system without growth-enhancing technology during feedlot finishing f: ADG: average daily gain;

Carbon footprint was mostly reported as environmental impacts in the LCA studies. A substantial range in CF is listed (Table 13 and Table 14) in the unit of kg CO_2e kg^{-1} carcass weight. Studies without a complete LCA analysis were excluded. Several LCA studies used different function unit, which was converted using a dressing percentage of 55%, and carcass cutting yield of 70%.

Due to various model assumptions, environmental condition, and methodological differences, conclusions cannot be drawn among beef LCA studies across global regions. For instance, a longer finishing time and higher cattle body weight approach was adopted in western Canadian beef production, which would lead to a relatively higher environmental impact (Lupo et al., 2013). A more typical example of different finishing timescale was seen in the Brazil case, where the CF reported to be more than 50% higher than it in the conventional US system (Cerri et al., 2016).

The carbon footprint of beef production ranged from 9.9 to 34.9 kg CO_2e kg^{-1} carcass weight from studies depending on the production system, location, cattle type, allocation, and system boundaries. To make the comparison, the CF values need to be categorized under the similar raising systems.

The 2-phase production system consisted of cow-calf and stocking/backgrounding phases referred to as grain-finished cattle in some cases. The CF for 2-phase systems were in the range of 18.9 to 26.9 kg CO_2e kg^{-1} carcass weight, with a median of 21.2 ± 4.12. An exceedingly low CF was reported by an Australia study of grain-finished cattle as in Peters et al., but note the cow-calf stage was excluded in this estimation (Peters et al., 2010). Conventional beef production is the most commonly used system in the US, some studies from outside the US also adapted their CF estimation based on the 3-phase system. The CF from 3-phase conventional production system ranged from 16 to 29.5 kg $CO_2e\ kg^{-1}$ carcass weight, with a median of 21.4 ± 4.29 kg $CO_2e\ kg^{-1}$ carcass weight. The stocking period slightly raised the GHG emission compare to the 2-phase system, but no significant differences were found. CF estimation from US grass-fed cattle system ranges from 25.05 to 34.9 kg $CO_2e\ kg^{-1}$ carcass weight, with a median of 31.6 kg $CO_2e\ kg^{-1}$ carcass weight. The CF from grass-fed cattle production in the US is significantly greater than both 2-phase production ($P<0.05$) and conventional production ($P=0.01$), it is roughly 42% and 45% higher than CF in 2-phase and 3-phase cattle production systems. Studies also indicated that the feedlot finished cattle carried a lower CF compare to grass-fed cattle (Capper, 2012; Lupo et al., 2013; Pelletier et al., 2010; Peters et al., 2010). Because the concentrated diet provided more digestible nutrients, which increase the weight-gaining speed. The shorter lifetime would then lead to less enteric methane emission. However, CF could be very dissimilar in feedlot finishing cattle based on the average age at which cows gave birth to their first calf (Ridoutt et al., 2011). A study based on Northern Great Plains farms (Lupo et al., 2013) used a shorter finishing time when estimate CF, the GHG emissions were 31.5 kg $CO_2e\ kg^{-1}$ hot carcass weight. Yet the shorter finishing time for grass-fed cattle implies a lighter finishing weight and a higher dressing percentage. Consequently, for the same amount of beef produced, the shorter finishing time on grass may not be the most sustainable strategy.

The EU studies often based on grass-fed or organic beef system which produce both beef and milk, while the US studies usually involve multiple operating systems. Grass-fed cattle system in EU has a CF lined from 15.6 to 19.9 kg $CO_2e\ kg^{-1}$ carcass weight, with a median of 18.2 ± 2.17 kg $CO_2e\ kg^{-1}$ carcass weight. It is highly relevant to mention farm types in explaining this CF elevation. More than half of the beef production farms in the EU were conjugated milk and beef production system (Cederberg and Stadig, 2003). When comparing with US farms, a great portion of CF burden in the EU farms was ascribed to the milk system. Figure 21 indicated the carbon footprint of the beef product under different raising system in EU and US. As mentioned, the 2-phase and 3-phase systems in the US presented a similar CF estimate, and grass-fed system in EU carries a notable low CF compare to it in the US.

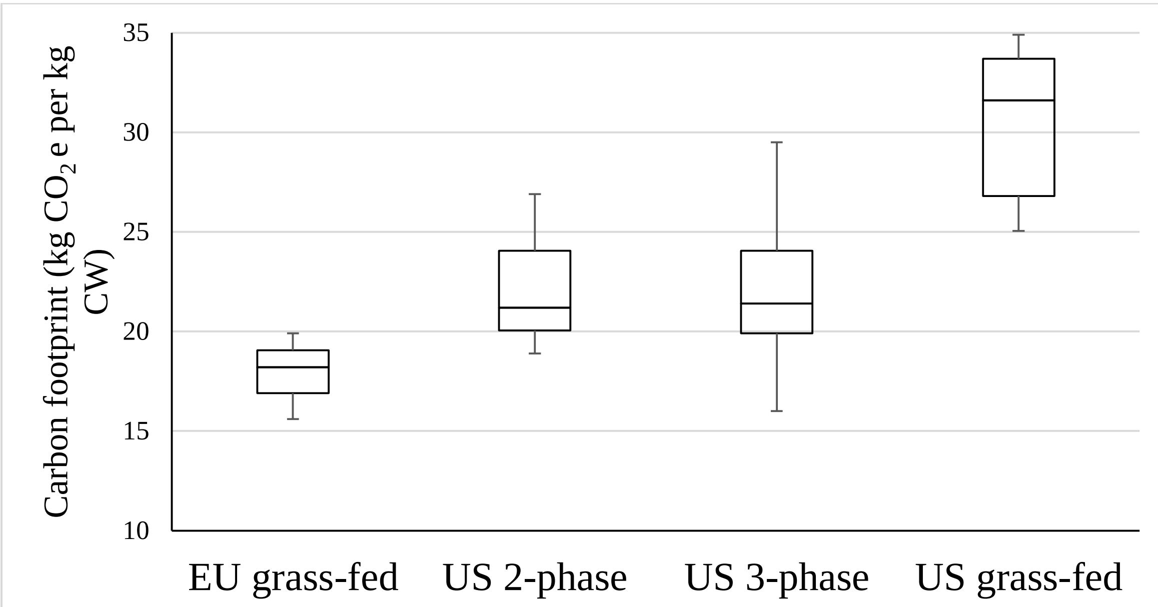

Figure 21 Beef production carbon footprint under different raising systems in EU and US

Commonly seen CF variations across literature may cause by disparate dressing percentage and beef yield convention rate. For instance, Ogino et al. (2007) reported environmental impacts of 36.4 kg CO_2e kg^{-1} beef from the cow-calf and fattening system, while the CF is 22.3 kg CO_2e kg^{-1} beef reported by Cederberg's et al. (2003). If GHG emissions from both studies converted to live weight based function unit, the figures become quite similar: 14.6 and 15.6 kg CO_2e kg^{-1} live weight, respectively. Therefore, the conversion rate in LCA studies should be clearly noted, and the original function unit should be reported.

LCA analysis has been used to evaluate the environmental impact of GHGs in recent years, an interesting tendency was observed based on the LCA study's timeline. For study focused on conventional beef production systems in the US, the latest study tended to have a lower CF value. Due to the limited number of studies, this tendency was only based on graphic observation. There are studies focused on environmental impact comparison between historical and modern operations. For example, Capper's (2011) project was targeting comparison between 1977 and 2007 beef production systems and concluded the sustainable agriculture improvements in a modern beef production system is crucial in order to meet the increasing population demand.

The LCA analysis also provided a breakdown of carbon footprint and identified the leading contributor under different scenarios. For the conventional beef production system, the cow-calf category is the well-defined leading impact because maintaining a cow is the most emission-intensive aspect in cattle production. Considering a cow could only produce one calf per year, the low fecundity raises the GHG emissions in this stage. In the 2-phase beef productions, cow-calf is still the largest contributor of the total GHG emissions. Enteric methane emission and manure management were the second leading contributors (Roop et al., 2014).

Table 15 CF breakdown from the literature based on beef production system

Production phases	*(Rotz et al., 2015)*	*(Rotz et al., 2013)*	*(Pelletier et al., 2010)*[b]	*(Pelletier et al., 2010)*	*(Lupo et al., 2013)*
Cow-calf	67.3%	71%	63% [c]	63% [c]	58%
Stocking	17.8%	—[a]	—	15.4%	—
Feedlot	14.9%	19%	23.5%	12.5%	—
Total CF[d]	22.2	19.84	26.9	29.5	23

a: not reported in the literature; b: 2-phase production system; c: averaged contribution between two production systems; d: Carbon footprint function unit: kg CO_2e kg^{-1} CW, Dressing percentage: 55%

Table 15 listed several studies with CF breakdown based on the production system. On average, about 64.5% of GHG emissions was contributed from the cow-calf phase, the CF contribution from stocking/backgrounding and feedlot was indistinct. This could be explained by individual growing period, feeding, and cattle breed etc.

The enteric methane fermentation was the major unit process contributor. It was held responsible for 39-41% CF within the cow-calf stage, and 73-88% in the feedlot stage (Nguyen et al., 2012). Published research suggested that the enteric methane emission was accounting for 31% to 66% of the total GHG emission from the system (Nguyen et al., 2012; Pelletier et al., 2010; Rotz et al., 2013; Rowntree et al., 2016; Veysset et al., 2010). This figure was even higher in the Japanese study, which 46-75% CF was due to enteric fermentation (Tsutsumi et al., 2018). And an Italian study raised the enteric methane contribution up to 75-85% of the total CF in a production similar to the conventional system in the US (Bragaglio et al., 2018). The high methane emission, in this case, was due to the use of forages rather than concentrates on feeding.

There are other major CF components reported in the LCA studies, such as feed production and manure management. In a conventional system with the CF 18.9 kg CO_2e kg^{-1} CW, feed production was the main contributor in feedlot phase, which accounted for 60-79% of the total CF (Roop et al., 2014). A study based on Italian beef operation reported a similar ratio. The fattening phase in Bragaglio's research is analog to the feedlot operations in the US system, and the feeding supplementation related GHG emission was accounting for 57% of the emission from the fattening stage. (Bragaglio et al., 2018). Dudley categorized the average GHG emission in the US beef production were found to be from pasture (43%), indirect land use change (25%), feedlot (20%), and crop production for feed (11%). (Dudley et al., 2014)

The grass-fed beef production revealed enteric methane as the leading GHG. Enteric methane was accounted for 57% of the total CF (33.7 kg CO_2e kg^{-1} CW); following by the 24% contribution of direct N_2O emission from grazed pastures (Tichenor et al., 2016).

2.4.4 Sensitivity analysis and uncertainty analysis

Sensitivity analysis was used to determine how different input variable impact the dependent CF value under a given assumption. Some studies also introduced sensitivity index, which is the ratio of the percent change in output over the percent change in input. For different system boundaries, Nguyen (2010) conducted the sensitivity analysis in the EU study to estimate the CF change if land opportunity cost and land use change related to grazing and feed crop production were taken into account. The CF would increase 3.1-3.9 per kg beef (CW) if both factors were included. Researchers believed this results highlighted the importance of considering land use impacts in assessing the environmental impacts of livestock production, and promoting sustainable land use is under urgent need. A research in the US also confirmed the land use change was the highest degree of uncertainty associated with beef production. Dudley et al. (2014) employed the change percentage in the sensitivity analysis and found indirect land use change was the most sensitive parameter in GHG emissions, which could change 500% carbon footprint in LCA studies. Other factors impact CF in the beef production system encompass pasture soil emissions (fertilizer, cattle backgrounding, grazing intensity etc.), manure management, and enteric fermentation. Dudley reported the N-excretion rate in manure management from the feedlot phase has the greatest influence on final emission, and the methane conversion factor (MCF) is most sensitive parameter within feedlot manure methane emissions (Dudley et al., 2014). In a regional scale, CF was moderately sensitive to enteric methane and slightly sensitive to emissions from purchased inputs and N_2O from pasture and crop (Rotz et al., 2015).

The Monte Carlo simulation is a technique converts uncertainties in input variables into probability distributions over output variables (Park, 2008). Uncertainty analysis quantifies the confidence in the predicted carbon footprints and was constructed using the Monte Carlo method in several LCA studies (Dudley et al., 2014; Lupo et al., 2013; Ruviaro et al., 2015).

2.5 Conclusions, limitation, and future work

Most existing beef LCA studies followed a "cradle to farm gate" approach and they reported CF from three typical raising systems: 2-phase, 3-phase, and grass-fed. Literature included in the present study used function unit of kg CO_2e kg^{-1} carcass weight. Emission factor calculations and LCA software were used in estimating carbon footprints. The most commonly used software is SimaPro and OpenLCA. SimaPro offers a great graphical representation, and OpenLCA brought cost-friendly access for researchers.

The CF from 2-phase production range from 18.9 to 26.9 kg CO_2e kg^{-1} carcass weight, with a median of 21.2 ± 4.12 kg CO_2e kg^{-1} carcass weight. The 3-phase raising system was the most-studied type, with CF range from 16 to 29.5 kg CO_2e kg^{-1} carcass weight, and a median of 21.4 ± 4.29 kg CO_2e kg^{-1} carcass weight. The highest CF was reported from grass-fed cattle systems in the U.S., due to methane production from pasture-based beef production. However, the CF from grass-fed cattle in EU was quite low, it ranged from 15.6 to 19.9 kg CO_2e kg^{-1} carcass weight, with a median of 18.2 ± 2.17 kg CO_2e kg^{-1} carcass weight. It could be explained by the agricultural type in the EU. There are more than 50% of farms produce both beef and milk, and the CF burden was then partaken by the dairy production.

Identifying the leading source of GHG emission from the beef production could indicate the mitigation priorities. The literature reported CF breakdowns based on raising system and unit produce factors. CF from the cow-calf stage is about three to four times higher than it from stocking/backgrounding and feedlot due to the low fecundity. The feedlot stage is the most intensive raising system, it carried the least GHG emissions. In another word, feedlot finished beef is less emission-intensive. Due to the high demand for food, feed production contributed the most in the feedlot phase if forages were applied rather than concentrates. Moreover, the methane conversion factor (MCF) is most sensitive in this stage.

The reported leading uncertainty source was land use change, which explained the suggestion from the literature of intensifying beef production system in mitigating GHG emissions. Moving towards intensive raising system and increase the efficiency of feed usage could reduce GHG emission from cradle to farm gate stage. In addition, combining dairy production with beef production also suggested a sustainable way of reducing CF.

Details about the cattle breed were not well defined in most published studies. Therefore, the cattle breed was neglected in categorizing cattle systems. Although beef CF after the farm gate occupied a smaller portion of the life cycle GHG emissions, it is quite helpful to include the CF from transportation and food waste into consideration. In addition, as a result of variations in cattle farm operations (raising period) and geographic conditions, developing a regional CF range is recommended.

References

Alexander, B., Hastings, M., Allman, D., Dachs, J., Thornton, J., & Kunasek, S. (2009). Quantifying atmospheric nitrate formation pathways based on a global model of the oxygen isotopic composition of atmospheric nitrate. *Atmospheric Chemistry and Physics, 9*(14), 5043-5056.

Anderson, R. R., Martello, D. V., Lucas, L. J., Davidson, C. I., Modey, W. K., & Eatough, D. J. (2006). Apportionment of ambient primary and secondary pollutants during a 2001 summer study in Pittsburgh using US Environmental Protection Agency UNMIX. *J Air Waste Manag Assoc, 56*(9), 1301-1319.

Andreini, E. M., & Place, S. E. (2014). Current approaches of beef cattle systems life cycle assessment: A review: Department of Animal Science. Oklahoma State University. White Paper: Sustainability.

Appel, B., Tokiwa, Y., Hsu, J., Kothny, E., & Hahn, E. (1985). Visibility as related to atmospheric aerosol constituents. *Atmospheric Environment (1967), 19*(9), 1525-1534.

Beauchemin, K. A., Henry Janzen, H., Little, S. M., McAllister, T. A., & McGinn, S. M. (2010). Life cycle assessment of greenhouse gas emissions from beef production in western Canada: A case study. *Agricultural Systems, 103*(6), 371-379. doi:http://dx.doi.org/10.1016/j.agsy.2010.03.008

Beauchemin, K. A., Janzen, H. H., Little, S. M., McAllister, T. A., & McGinn, S. M. (2011). Mitigation of greenhouse gas emissions from beef production in western Canada - Evaluation using farm-based life cycle assessment. *Animal Feed Science and Technology, 166-67*, 663-677. doi:DOI 10.1016/j.anifeedsci.2011.04.047

Bragaglio, A., Napolitano, F., Pacelli, C., Pirlo, G., Sabia, E., Serrapica, F., . . . Braghieri, A. (2018). Environmental impacts of Italian beef production: A comparison between different systems. *Journal of Cleaner Production, 172*, 4033-4043. doi:10.1016/j.jclepro.2017.03.078

Brimblecombe, P. (1981). Long term trends in London fog. *Science of the Total Environment, 22*(1), 19-29. doi:http://dx.doi.org/10.1016/0048-9697(81)90078-4

Brown, S. G., Eberly, S., Paatero, P., & Norris, G. A. (2015). Methods for estimating uncertainty in PMF solutions: Examples with ambient air and water quality data and guidance on reporting PMF results. *Science of the Total Environment, 518*, 626-635. doi:10.1016/j.scitotenv.2015.01.022

Capper, J. L. (2011). The environmental impact of beef production in the United States: 1977 compared with 2007. *J Anim Sci, 89*(12), 4249-4261.

Capper, J. L. (2012). Is the grass always greener? Comparing the environmental impact of conventional, natural and grass-fed beef production systems. *Animals, 2*(2), 127-143.

Casey, J., & Holden, N. (2006). Quantification of GHG emissions from sucker-beef production in Ireland. *Agricultural Systems, 90*(1), 79-98. doi:https://doi.org/10.1016/j.agsy.2005.11.008

Cederberg, C., & Stadig, M. (2003). System expansion and allocation in life cycle assessment of milk and beef production. *The International Journal of Life Cycle Assessment, 8*(6), 350-356.

Cerri, C. C., Moreira, C. S., Alves, P. A., Raucci, G. S., de Almeida Castigioni, B., Mello, F. F. C., . . . Cerri, C. E. P. (2016). Assessing the carbon footprint of beef cattle in Brazil: a case study with 22 farms in the State of Mato Grosso. *Journal of Cleaner Production, 112*, 2593-2600. doi:https://doi.org/10.1016/j.jclepro.2015.10.072

Chan, Y., Simpson, R., Mctainsh, G. H., Vowles, P. D., Cohen, D., & Bailey, G. (1999). Source apportionment of visibility degradation problems in Brisbane (Australia) using the multiple linear regression techniques. *Atmospheric Environment, 33*(19), 3237-3250.

Chen, F., Miao, S., Tewari, M., Bao, J. W., & Kusaka, H. (2011). A numerical study of interactions between surface forcing and sea breeze circulations and their effects on stagnation in the greater Houston area. *Journal of Geophysical Research: Atmospheres, 116*(D12).

Cornell University. (2012). Yields and dressing percentages. *Cornell small farms program.* Retrieved from http://smallfarms.cornell.edu/2012/07/10/yields-and-dressing-percentages/

Crosson, P., Shalloo, L., O'Brien, D., Lanigan, G. J., Foley, P. A., Boland, T. M., & Kenny, D. A. (2011). A review of whole farm systems models of greenhouse gas emissions from beef and dairy cattle production systems. *Animal Feed Science and Technology, 166-167*, 29-45. doi:https://doi.org/10.1016/j.anifeedsci.2011.04.001

Davis, R. E. (1991). A synoptic climatological analysis of winter visibility trends in the mideastern United States. *Atmospheric Environment. Part B. Urban Atmosphere, 25*(2), 165-175.

de Vries, M., & de Boer, I. (2010). Comparing environmental impacts for livestock products: A review of life cycle assessments. *Livestock Science, 128*(1), 1-11.

Desjardins, R. L., Worth, D. E., Vergé, X. P., Maxime, D., Dyer, J., & Cerkowniak, D. (2012). Carbon footprint of beef cattle. *Sustainability, 4*(12), 3279-3301.

Dick, M., Abreu da Silva, M., & Dewes, H. (2015). Life cycle assessment of beef cattle production in two typical grassland systems of southern Brazil. *Journal of Cleaner Production, 96*, 426-434. doi:http://dx.doi.org/10.1016/j.jclepro.2014.01.080

Doyle, M., & Dorling, S. (2002). Visibility trends in the UK 1950–1997. *Atmospheric Environment, 36*(19), 3161-3172. doi:http://dx.doi.org/10.1016/S1352-2310(02)00248-0

Dudley, Q. M., Liska, A. J., Watson, A. K., & Erickson, G. E. (2014). Uncertainties in lifecycle greenhouse gas emissions from U.S. beef cattle. *Journal of Cleaner Production, 75*, 31-39. doi:10.1016/j.jclepro.2014.03.087

Eatough, D. J., Anderson, R. R., Martello, D. V., Modey, W. K., & Mangelson, N. E. (2006). Apportionment of ambient primary and secondary PM2.5 during a 2001 summer intensive study at the NETL Pittsburgh site using PMF2 and EPA UNMIX. *Aerosol science and technology, 40*(10), 925-940. doi:10.1080/02786820600796616

Efron, B., & Tibshirani, R. J. (1993). An Introduction to the Bootstrap, Monographs on Statistics and Applied Probability, Vol. 57. *New York and London: Chapman and Hall/CRC*.

Engel-Cox, J. A., & Weber, S. A. (2007). Compilation and assessment of recent positive matrix factorization and UNMIX receptor model studies on fine particulate matter source apportionment for the eastern United States. *J Air Waste Manag Assoc, 57*(11), 1307-1316. doi:10.3155/1047-3289.57.11.1307

Environmental Working Group. (2011). Meat Eater's Guide to Climate Change and Health: Environmental Working Group, Washington, DC.

EPA. (1979). Visibility Protecting: an EPA Report to Congress. *US Environmental Protection Agency: Research Triangle Park, NC*.

EPA. (1995). *Compilation of air pollutant emission factors* (Fifth ed.).

EPA. (2016). Receptor Modeling. *Support Center for Regulatory Atmospheric Modeling(SCRAM).* Retrieved from https://www3.epa.gov/ttn/scram/receptorindex.htm

EPA. (2018). Inventory of US Greenhouse Gas Emissions and Sinks: 1990–2016. *Washington, DC, USA, EPA.*

Ethirajan, R., & Mohan, S. (2012). Comparative Evaluation of VOC Source Profiles Developed by PMF and UNMIX Models. *International Journal of Environmental Science and Development, 3*(5), 450.

FAO. (2014). Agriculture's greenhouse gas emissions on the rise. Retrieved from http://www.fao.org/news/story/en/item/216137/icode/

Flachowsky, G., Meyer, U., & Sudekum, K. H. (2018). Invited review: Resource inputs and land, water and carbon footprints from the production of edible protein of animal origin. *Archives Animal Breeding, 61*(1), 17-36. doi:10.5194/aab-61-17-2018

Ghim, Y. S., Moon, K.-C., Lee, S., & Kim, Y. P. (2005). Visibility Trends in Korea during the Past Two Decades. *J Air Waste Manag Assoc, 55*(1), 73-82. doi:10.1080/10473289.2005.10464599

Gultepe, I., & Isaac, G. (2006). *Visibility versus precipitation rate and relative humidity.* Paper presented at the Preprints, 12th Cloud Physics Conf., Madison, WI, Amer. Meteor. Soc. P.

Gupta, I., Salunkhe, A., & Kumar, R. (2012). Source apportionment of PM_{10} by positive matrix factorization in urban area of Mumbai, India. *The Scientific World Journal, 2012*.

Heller, M. C., & Keoleian, G. A. (2011). Life Cycle Energy and Greenhouse Gas Analysis of a Large-Scale Vertically Integrated Organic Dairy in the United States. *Environmental science & technology, 45*(5), 1903-1910. doi:10.1021/es102794m

Henneman, L. R., Holmes, H. A., Mulholland, J. A., & Russell, A. G. (2015). Meteorological detrending of primary and secondary pollutant concentrations: Method application and evaluation using long-term (2000–2012) data in Atlanta. *Atmospheric Environment, 119*, 201-210.

Henry, R. C. (2003). Multivariate receptor modeling by N-dimensional edge detection. *Chemometrics and Intelligent Laboratory Systems, 65*(2), 179-189. doi:Doi 10.1016/S0169-7439(02)00108-9

Hu, S., McDonald, R., Martuzevicius, D., Biswas, P., Grinshpun, S. A., Kelley, A., . . . LeMasters, G. (2006). UNMIX modeling of ambient PM 2.5 near an interstate highway in Cincinnati, OH, USA. *Atmospheric Environment, 40*, 378-395.

Huang, X., Liu, Z., Zhang, J., Wen, T., Ji, D., & Wang, Y. (2016). Seasonal variation and secondary formation of size-segregated aerosol water-soluble inorganic ions during pollution episodes in Beijing. *Atmospheric Research, 168*(Supplement C), 70-79. doi:https://doi.org/10.1016/j.atmosres.2015.08.021

Hubbell, B. J., Crume, R. V., Evarts, D. M., & Cohen, J. M. (2010). Policy Monitor Regulation and Progress under the 1990 Clean Air Act Amendments. *Review of Environmental Economics and Policy, 4*(1), 122-138.

Intergovernmental Panel On Climate Change. (2007). *IPCC Fourth Assessment Report: Climate Change 2007 (AR4)*. IPCC: Cambridge, UK.

ISO. (1997). *Environmental Management: Life Cycle Assessment: Principles and Framework* (Vol. 14040): ISO.

ISO. (2006). *Environmental management–life cycle assessment–principles and framework*. London: British Standards Institution.

Jeong, C.-H., Wang, J. M., & Evans, G. J. (2016). Source Apportionment of Urban Particulate Matter using Hourly Resolved Trace Metals, Organics, and Inorganic Aerosol Components. *Atmos. Chem. Phys. Discuss.*

Johnson, R. J. (2010). Livestock, Dairy, and Poultry Outlook. *Economic Research Service, United States Department of Agriculture*.

Kansas Department of Health and Environment. (2010). *State of Kansas Flint Hills Smoke Management Plan*. Retrieved from http://www.kdheks.gov/bar/air-monitor/flinthillsinfo/SMP_v10FINAL.pdf.

Katzman, T. L., Rutter, A. P., Schauer, J. J., Lough, G. C., Kolb, C. J., & Van Klooster, S. (2010). $PM_{2.5}$ and $PM_{10-2.5}$ Compositions during Wintertime Episodes of Elevated PM Concentrations across the Midwestern USA. *Aerosol and Air Quality Research, 10*(2), 140-153. doi:10.4209/aaqr.2009.10.0063

Ke, H. H., Ondov, J. M., & Rogge, W. F. (2013). Detailed emission profiles for on-road vehicles derived from ambient measurements during a windless traffic episode in Baltimore using a multi-model approach. *Atmospheric Environment, 81*, 280-287. doi:10.1016/j.atmosenv.2013.08.020

Khodeir, M., Shamy, M., Alghamdi, M., Zhong, M., Sun, H., Costa, M., . . . Maciejczyk, P. (2012). Source apportionment and elemental composition of $PM_{2.5}$ and PM_{10} in Jeddah City, Saudi Arabia. *Atmospheric Pollution Research, 3*(3), 331-340.

Kim, Hopke, P. K., Larson, T. V., & Covert, D. S. (2004). Analysis of ambient particle size distributions using unmix and positive matrix factorization. *Environmental science & technology, 38*(1), 202-209. doi:10.1021/es030310s

Kim, Y. J., Spak, S. N., Carmichael, G. R., Riemer, N., & Stanier, C. O. (2014). Modeled aerosol nitrate formation pathways during wintertime in the Great Lakes region of North America. *Journal of Geophysical Research-Atmospheres, 119*(21), 12420-12445. doi:10.1002/2014jd022320

Kreidenweis, S. M., Remer, L. A., Bruintjes, R., & Dubovik, O. (2001). Smoke aerosol from biomass burning in Mexico: Hygroscopic smoke optical model. *Journal of Geophysical Research: Atmospheres, 106*(D5), 4831-4844. doi:10.1029/2000JD900488

Kundu, S., & Stone, E. A. (2014). Composition and sources of fine particulate matter across urban and rural sites in the Midwestern United States. *Environmental Science: Processes & Impacts, 16*(6), 1360-1370.

Lang, Y.-H., Li, G.-L., Wang, X.-M., Peng, P., & Bai, J. (2015). Combination of Unmix and positive matrix factorization model identifying contributions to carcinogenicity and mutagenicity for polycyclic aromatic hydrocarbons sources in Liaohe delta reed wetland soils, China. *Chemosphere, 120*, 431-437. doi:10.1016/j.chemosphere.2014.08.048

Latha, K. M., & Badarinath, K. (2003). Black carbon aerosols over tropical urban environment—a case study. *Atmospheric Research, 69*(1), 125-133.

Lawson, D. R. (1998). *Northern Front Range Air Quality Study*. Retrieved from

Lee, C.-T., & Cheng, J.-P. (1996). The effects of aerosol species and meteorological factors on visibility in the Taipei metropolitan area. *J. CHIN. INST. ENVIRON. ENG., 6*(1), 21-30.

Lee, E., Chan, C. K., & Paatero, P. (1999). Application of positive matrix factorization in source apportionment of particulate pollutants in Hong Kong. *Atmospheric Environment, 33*(19), 3201-3212. doi:http://dx.doi.org/10.1016/S1352-2310(99)00113-2

Lewis, C. W., Norris, G. A., Conner, T. L., & Henry, R. C. (2003). Source apportionment of Phoenix $PM_{2.5}$ aerosol with the Unmix receptor model. *J Air Waste Manag Assoc, 53*(3), 325-338.

Lewtas, J., Maykut, N., Kim, E., & Larson, T. (2002). *Improving source profiles and apportionment of combustion sources using thermal carbon fractions in multuvariate receptor models.* Paper presented at the American Association for Aerosol Research, Charlotte, NC.

Liu, Z., Liu, Y., Maghirang, R., Devlin, D., & Blocksome, C. (2016). Estimating Contributions of Prescribed Rangeland Burning in Kansas to Ambient PM2. 5 through Source Apportionment with the Unmix Receptor Model. *Transactions of the ASABE, 59*(5), 1267-1275.

López, M. L., Ceppi, S., Palancar, G. G., Olcese, L. E., Tirao, G., & Toselli, B. M. (2011). Elemental concentration and source identification of PM10 and PM2. 5 by SR-XRF in Córdoba City, Argentina. *Atmospheric Environment, 45*(31), 5450-5457.

Lupo, C. D., Clay, D. E., Benning, J. L., & Stone, J. J. (2013). Life-Cycle Assessment of the Beef Cattle Production System for the Northern Great Plains, USA. *J Environ Qual, 42*, 1386-1394. doi:10.2134/jeq2013.03.0101

Ma, Y., Weber, R., Lee, Y.-N., Orsini, D., Maxwell-Meier, K., Thornton, D., . . . Sachse, G. (2003). Characteristics and influence of biosmoke on the fine-particle ionic composition measured in Asian outflow during the Transport and Chemical Evolution over the Pacific (TRACE-P) experiment: NASA global tropospheric experiment transport and chemical evolution over the pacific (TRACE-P): Measurements and analysis (TRACEP1). *Journal of geophysical research, 108*(D21), GTE37. 31-GTE37. 16.

Malm, W. C., & Day, D. E. (2001). Estimates of aerosol species scattering characteristics as a function of relative humidity. *Atmospheric Environment, 35*(16), 2845-2860.

Maykut, N. N., Lewtas, J., Kim, E., & Larson, T. V. (2003). Source apportionment of $PM_{2.5}$ at an urban IMPROVE site in Seattle, Washington. *Environmental science & technology, 37*(22), 5135-5142. doi:10.1021/es030370y

Mijic, Z., Stojic, A., Perisic, M., Rajsic, S., & Tasic, M. (2012). Receptor Modeling Studies for the Characterization of Pm10 Pollution Sources in Belgrade. *Chemical Industry & Chemical Engineering Quarterly, 18*(4), 623-634. doi:10.2298/Ciceq120104108m

Miller, S. L., Anderson, M. J., Daly, E. P., & Milford, J. B. (2002). Source apportionment of exposures to volatile organic compounds. I. Evaluation of receptor models using simulated exposure data. *Atmospheric Environment, 36*(22), 3629-3641. doi:10.1016/S1352-2310(02)00279-0

Mogensen, L., Kristensen, T., Nielsen, N. I., Spleth, P., Henriksson, M., Swensson, C., . . . Vestergaard, M. (2015). Greenhouse gas emissions from beef production systems in Denmark and Sweden. *Livestock Science, 174*, 126-143. doi:http://dx.doi.org/10.1016/j.livsci.2015.01.021

Montes, F., Meinen, R., Dell, C., Rotz, A., Hristov, A., Oh, J., . . . Makkar, H. (2013). SPECIAL TOPICS—mitigation of methane and nitrous oxide emissions from animal operations: II. A review of manure management mitigation options. *J Anim Sci, 91*(11), 5070-5094.

National Research Council. (1999). *Research Priorities for Airborne Particulate Matter: II. Evaluating Research Progress and Updating the Portfolio* (Vol. 2): National Academies Press.

Ng, N. L., Kroll, J. H., Keywood, M. D., Bahreini, R., Varutbangkul, V., Flagan, R. C., . . . Goldstein, A. H. (2006). Contribution of first- versus second-generation products to secondary organic aerosols formed in the oxidation of biogenic hydrocarbons. *Environ Sci Technol, 40*(7), 2283-2297.

Nguyen, T. L. T., Hermansen, J. E., & Mogensen, L. (2010). Environmental consequences of different beef production systems in the EU. *Journal of Cleaner Production, 18*(8), 756-766.

Nguyen, T. T. H., Van der Werf, H., Eugène, M., Veysset, P., Devun, J., Chesneau, G., & Doreau, M. (2012). Effects of type of ration and allocation methods on the environmental impacts of beef-production systems. *Livestock Science*, *145*(1), 239-251.

Norris, Vedantham, R., Duvall, R., & Henry, R. (2007). EPA Unmix 6.0 fundamentals & user guide. *US Environmental Protection Agency, Office of Research and Development, Washington, DC, 20460*.

Norris, G., Vedantham, R., Wade, K., Zahn, P., Brown, S., Paatero, P., . . . Martin, L. (2009). Guidance document for PMF applications with the Multilinear Engine. *Prepared for the US Environmental Protection Agency, Research Triangle Park, NC, by the National Exposure Research Laboratory, Research Triangle Park, NC*.

Ogino, A., Kaku, K., Osada, T., & Shimada, K. (2004). Environmental impacts of the Japanese beef-fattening system with different feeding lengths as evaluated by a life-cycle assessment method 1. *J Anim Sci*, *82*(7), 2115-2122.

Ogino, A., Orito, H., Shimada, K., & Hirooka, H. (2007). Evaluating environmental impacts of the Japanese beef cow–calf system by the life cycle assessment method. *Animal Science Journal*, *78*(4), 424-432.

Paatero, P., & Tapper, U. (1994). Positive matrix factorization: A non - negative factor model with optimal utilization of error estimates of data values. *Environmetrics*, *5*(2), 111-126. doi:10.1002/env.3170050203

Pandey, D., Agrawal, M., & Pandey, J. S. (2011). Carbon footprint: current methods of estimation. *Environmental monitoring and assessment*, *178*(1-4), 135-160.

Pandolfi, M., Gonzalez-Castanedo, Y., Alastuey, A., de la Rosa, J. D., Mantilla, E., de la Campa, A. S., . . . Moreno, T. (2011). Source apportionment of PM10 and PM2.5 at multiple sites in the strait of Gibraltar by PMF: impact of shipping emissions. *Environmental Science and Pollution Research*, *18*(2), 260-269. doi:10.1007/s11356-010-0373-4

Park, J. (2008). *Assessing Climate Change under Uncertainty: A Monte Carlo Approach.* Citeseer.

Park, R. J., Jacob, D. J., & Logan, J. A. (2007). Fire and biofuel contributions to annual mean aerosol mass concentrations in the United States. *Atmospheric Environment*, *41*(35), 7389-7400. doi:10.1016/j.atmosenv.2007.05.061

Pekney, Davidson, Robinson, Zhou, L., Hopke, P., Eatough, D., & Rogge, W. F. (2006a). Major source categories for PM2. 5 in Pittsburgh using PMF and UNMIX. *Aerosol science and technology*, *40*(10), 910-924.

Pekney, N. J., Davidson, C. I., Zhou, L., & Hopke, P. K. (2006b). Application of PSCF and CPF to PMF-modeled sources of PM2. 5 in Pittsburgh. *Aerosol science and technology*, *40*(10), 952-961.

Pelletier, N., Pirog, R., & Rasmussen, R. (2010). Comparative life cycle environmental impacts of three beef production strategies in the Upper Midwestern United States. *Agricultural Systems*, *103*(6), 380-389. doi:http://dx.doi.org/10.1016/j.agsy.2010.03.009

Peters, G. M., Rowley, H. V., Wiedemann, S., Tucker, R., Short, M. D., & Schulz, M. (2010). Red meat production in Australia: life cycle assessment and comparison with overseas studies. *Environmental science & technology*, *44*(4), 1327-1332.

Phetteplace, H. W., Johnson, D. E., & Seidl, A. F. (2001). Greenhouse gas emissions from simulated beef and dairy livestock systems in the United States. *Nutrient Cycling in Agroecosystems*, *60*(1), 99-102.

Pitchford, M. L., Poirot, R. L., Schichtel, B. A., & Maim, W. C. (2009). Characterization of the winter midwestern particulate nitrate bulge. *J Air Waste Manag Assoc*, *59*(9), 1061-1069.

Poirot, R. L., Wishinski, P. R., Hopke, P. K., & Polissar, A. V. (2001). Comparative application of multiple receptor methods to identify aerosol sources in northern Vermont. *Environmental science & technology, 35*(23), 4622-4636.

Rai, P., Chakraborty, A., Mandariya, A. K., & Gupta, T. (2016). Composition and source apportionment of PM1 at urban site Kanpur in India using PMF coupled with CBPF. *Atmospheric Research, 178–179*, 506-520. doi:10.1016/j.atmosres.2016.04.015

Rasmussen, R. M., Vivekanandan, J., Cole, J., Myers, B., & Masters, C. (1999). The estimation of snowfall rate using visibility. *Journal of Applied Meteorology, 38*(10), 1542-1563.

Rice, G., Clift, R., & Burns, R. (1997). Comparison of currently available european LCA software. *The International Journal of Life Cycle Assessment, 2*(1), 53-59.

Ridoutt, B. G., Sanguansri, P., & Harper, G. S. (2011). Comparing carbon and water footprints for beef cattle production in Southern Australia. *Sustainability, 3*(12), 2443-2455.

Roop, D. J., Shrestha, D. S., & Saul, D. A. (2013). Cradle-to-gate life cycle assessment of locally produced beef in the Palouse region of the Northwestern U.S. *Transactions of the ASABE, 56*(5), 1933-1941. doi:10.13031/trans.56.10122

Roop, D. J., Shrestha, D. S., Saul, D. A., & Newman, S. (2014). Cradle-to-gate life cycle assessment of regionally produced beef in the northwestern U.S. *Transactions of the ASABE, 57*(3), 927-935. doi:10.13031/trans.57.10498

Röös, E., Sundberg, C., Tidåker, P., Strid, I., & Hansson, P.-A. (2013). Can carbon footprint serve as an indicator of the environmental impact of meat production? *Ecological Indicators, 24*, 573-581.

Rotz, C., Isenberg, B., Stackhouse-Lawson, K., & Pollak, E. (2013). A simulation-based approach for evaluating and comparing the environmental footprints of beef production systems. *J Anim Sci, 91*(11), 5427-5437.

Rotz, C., Montes, F., & Chianese, D. (2010). The carbon footprint of dairy production systems through partial life cycle assessment. *J Dairy Sci, 93*(3), 1266-1282.

Rotz, C. A., Asem-Hiablie, S., Dillon, J., & Bonifacio, H. (2015). Cradle-to-farm gate environmental footprints of beef cattle production in Kansas, Oklahoma, and Texas. *J Anim Sci, 93*, 2509-2519. doi:10.2527/jas.2014-8809

Rowntree, J. E., Ryals, R., DeLonge, M. S., Teague, W. R., Chiavegato, M. B., Byck, P., . . . Xu, S. (2016). Potential mitigation of midwest grass-finished beef production emissions with soil carbon sequestration in the United States of America. *Future of Food: Journal on Food, Agriculture and Society, 4*(3), 31-38.

Roy, P., Nei, D., Orikasa, T., Xu, Q., Okadome, H., Nakamura, N., & Shiina, T. (2009). A review of life cycle assessment (LCA) on some food products. *Journal of Food Engineering, 90*(1), 1-10. doi:http://dx.doi.org/10.1016/j.jfoodeng.2008.06.016

Ruviaro, C. F., de Léis, C. M., Lampert, V. d. N., Barcellos, J. O. J., & Dewes, H. (2015). Carbon footprint in different beef production systems on a southern Brazilian farm: a case study. *Journal of Cleaner Production*. doi:10.1016/j.jclepro.2014.01.037

Scheehle, E., Godwin, D., Ottinger, D., & DeAngelo, B. (2006). Global anthropogenic non-CO2 greenhouse gas emissions: 1990–2020. *Version: revised June*.

Seinfeld, J. H., & Pandis, S. N. (2016). *Atmospheric chemistry and physics: from air pollution to climate change*: John Wiley & Sons.

Solomon, P. A., Crumpler, D., Flanagan, J. B., Jayanty, R., Rickman, E. E., & McDade, C. E. (2014). US National PM2. 5 Chemical Speciation Monitoring Networks—CSN and IMPROVE: Description of networks. *J Air Waste Manag Assoc, 64*(12), 1410-1438.

Song, Xie, Zhang, Y. H., Zeng, L. M., Salmon, L. G., & Zheng, M. (2006a). Source apportionment of $PM_{2.5}$ in Beijing using principal component analysis/absolute principal component scores and UNMIX. *Science of the Total Environment, 372*(1), 278-286. doi:10.1016/j.scitotenv.2006.08.041

Song, Y., Dai, W., Shao, M., Liu, Y., Lu, S., Kuster, W., & Goldan, P. (2008). Comparison of receptor models for source apportionment of volatile organic compounds in Beijing, China. *Environmental Pollution, 156*(1), 174-183. doi:10.1016/j.envpol.2007.12.014

Song, Y., Zhang, Y., Xie, S., Zeng, L., Zheng, M., Salmon, L. G., . . . Slanina, S. (2006b). Source apportionment of $PM_{2.5}$ in Beijing by positive matrix factorization. *Atmospheric Environment, 40*(8), 1526-1537. doi:10.1016/j.atmosenv.2005.10.039

Stackhouse-Lawson, K. R., Rotz, C. A., Oltjen, J. W., & Mitloehner, F. M. (2012). Carbon footprint and ammonia emissions of California beef production systems. *J Anim Sci, 90*, 4641-4655. doi:10.2527/jas.2011-4653

Stackhouse, K. R., Rotz, C. A., Oltjen, J. W., & Mitloehner, F. M. (2012). Growth-promoting technologies decrease the carbon footprint, ammonia emissions, and costs of california beef production systems. *J Anim Sci, 90*(12), 4656-4665. doi:10.2527/jas.2011-4654

Stanier, C., Singh, A., Adamski, W., Baek, J., Caughey, M., Carmichael, G., . . . Oleson, J. (2012). Overview of the LADCO winter nitrate study: hourly ammonia, nitric acid and PM 2.5 composition at an urban and rural site pair during PM 2.5 episodes in the US Great Lakes region. *Atmospheric Chemistry and Physics, 12*(22), 11037-11056.

Stewart, A., Little, S., Ominski, K., Wittenberg, K., & Janzen, H. (2009). Evaluating greenhouse gas mitigation practices in livestock systems: an illustration of a whole-farm approach. *The Journal of Agricultural Science, 147*(4), 367-382.

Subak, S. (1999). Global environmental costs of beef production. *Ecological Economics, 30*(1), 79-91.

Thomassen, M. A., Dalgaard, R., Heijungs, R., & De Boer, I. (2008). Attributional and consequential LCA of milk production. *The International Journal of Life Cycle Assessment, 13*(4), 339-349.

Tiao, G., Box, G., & Hamming, W. (1975). Analysis of Los Angeles photochemical smog data: a statistical overview. *Journal of the Air Pollution Control Association, 25*(3), 260-268.

Tichenor, N. E., Peters, C. J., Norris, G. A., Thoma, G., & Griffin, T. S. (2016). Life cycle environmental consequences of grass-fed and dairy beef production systems in the Northeastern United States. *Journal of Cleaner Production, 142*, 1619-1628. doi:http://dx.doi.org/10.1016/j.jclepro.2016.11.138

Towne, E. G., & Craine, J. M. (2014). Ecological Consequences of Shifting the Timing of Burning Tallgrass Prairie. *PLoS One, 9*(7), 103423. doi:10.1371/journal.pone.0103423

Tsai, Y. I., & Cheng, M. T. (1999). Visibility and aerosol chemical compositions near the coastal area in central Taiwan. *Science of the Total Environment, 231*(1), 37-51.

Tsutsumi, M., Ono, Y., Ogasawara, H., & Hojito, M. (2018). Life-cycle impact assessment of organic and non-organic grass-fed beef production in Japan. *Journal of Cleaner Production, 172*, 2513-2520. doi:10.1016/j.jclepro.2017.11.159

Turpin, B. J., & Huntzicker, J. J. (1995). Identification of secondary organic aerosol episodes and quantitation of primary and secondary organic aerosol concentrations during SCAQS. *Atmospheric Environment, 29*(23), 3527-3544.

United States Bureau of Land Management, I. F. D. (2008). *Proposed fire, fuels, and related vegetation management direction plan amendment and final environmental impact* *statement a regional assessment for southeast and south central Idaho*: U.S. Department of the Interior, Bureau of Land Management, Idaho Falls District.

Veysset, P., Lherm, M., & Bébin, D. (2010). Energy consumption, greenhouse gas emissions and economic performance assessments in French Charolais suckler cattle farms: model-based analysis and forecasts. *Agricultural Systems*, *103*(1), 41-50.

Wang, D., Zhou, B., Fu, Q., Zhao, Q., Zhang, Q., Chen, J., . . . Li, J. (2016). Intense secondary aerosol formation due to strong atmospheric photochemical reactions in summer: observations at a rural site in eastern Yangtze River Delta of China. *Science of the Total Environment*, *571*(Supplement C), 1454-1466. doi:https://doi.org/10.1016/j.scitotenv.2016.06.212

Watson. (2002). Visibility: Science and regulation. *J Air Waste Manag Assoc*, *52*(6), 628-713.

Watson, Chow, J., & Fujita, E. (1994). *Aerosol data validation for the 1992-93 Tucson Urban Haze Study*.

Watson, Chow, J. C., & Houck, J. E. (2001). PM2.5 chemical source profiles for vehicle exhaust, vegetative burning, geological material, and coal burning in Northwestern Colorado during 1995. *Chemosphere*, *43*(8), 1141-1151. doi:https://doi.org/10.1016/S0045-6535(00)00171-5

White, R. R., & Capper, J. L. (2013). An environmental, economic, and social assessment of improving cattle finishing weight or average daily gain within US beef production. *J Anim Sci*, *91*(12), 5801-5812. doi:10.2527/jas.2013-6632

Williams, A., Audsley, E., & Sandars, D. (2006). Determining the environmental burdens and resource use in the production of agricultural and horticultural commodities: Defra project report IS0205. *Zu finden in: http://randd. defra. gov. uk/Default. aspx*.

Wulf, D. M., Weight, C., & Weight, L. (1999). Did the locker plant steal some of my meat? *Brookings, SD: South Dakota State University*, 599-639.

Zhang, R., Wang, M., Sheng, L., Kanai, Y., & Ohta, A. (2004). Seasonal characterization of dust days, mass concentration and dry deposition of atmospheric aerosols over Qingdao, China. *China Particuology*, *2*(5), 196-199.

Zhao, H., Che, H., Zhang, X., Ma, Y., Wang, Y., Wang, H., & Wang, Y. (2013). Characteristics of visibility and particulate matter (PM) in an urban area of Northeast China. *Atmospheric Pollution Research*, *4*(4), 427-434. doi:http://dx.doi.org/10.5094/APR.2013.049

Zheng, M., Salmon, L. G., Schauer, J. J., Zeng, L., Kiang, C., Zhang, Y., & Cass, G. R. (2005). Seasonal trends in PM2. 5 source contributions in Beijing, China. *Atmospheric Environment*, *39*(22), 3967-3976.